NASA TECHNICAL NOTE

NASA TN D-1883

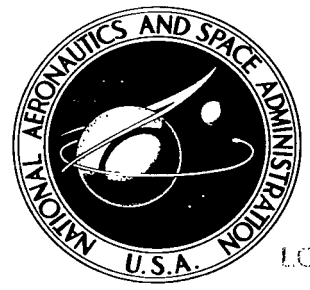

NASA TN D-1883

ANALYTICAL AND EXPERIMENTAL STUDY OF POOL HEATING OF LIQUID HYDROGEN OVER A RANGE OF ACCELERATIONS

by Robert W. Graham, Robert C. Hendricks, and Robert C. Ehlers

Lewis Research Center
Cleveland, Ohio

NATIONAL AERONAUTICS AND SPACE ADMINISTRATION • WASHINGTON, D. C. • FEBRUARY 1965

NASA TN D-1883

ANALYTICAL AND EXPERIMENTAL STUDY OF POOL HEATING OF LIQUID HYDROGEN OVER A RANGE OF ACCELERATIONS

By Robert W. Graham, Robert C. Hendricks,
and Robert C. Ehlers

Lewis Research Center
Cleveland, Ohio

Technical Film Supplement C-224 available on request

NATIONAL AERONAUTICS AND SPACE ADMINISTRATION

For sale by the Office of Technical Services, Department of Commerce,
Washington, D.C. 20230 -- Price $3.00

ANALYTICAL AND EXPERIMENTAL STUDY OF POOL HEATING OF LIQUID HYDROGEN OVER A RANGE OF ACCELERATIONS

by Robert W. Graham, Robert C. Hendricks, and Robert C. Ehlers

Lewis Research Center

SUMMARY

Pool heating of liquid hydrogen in the subcritical and supercritical pressure states has been investigated at Earth gravity and multigravities. Acceleration does influence the incipience of nucleate boiling but does not affect established nucleate boiling. The film-boiling heat transfer is influenced by multi-g accelerations.

A mechanism similar to boiling was evident for hydrogen in the supercritical and near-critical state. Acceleration magnitude influenced the heat transfer in this fluid regime. High-speed motion pictures of the heat-transfer processes were taken in both the subcritical and supercritical pressure states at Earth gravity and multigravities.

INTRODUCTION

Pool heating of cryogenic fluids, and particularly liquid hydrogen, can be encountered in numerous space vehicle design applications. Such a vehicle may experience a variety of body accelerations, which can range from zero to 10 or more g's. Consequently, information on the manner in which the local gravity influences heat transfer is needed. In addition, the observed gravitational effects on the heat transfer of any fluid are useful in evaluating conceptual models of such processes as nucleate and film boiling.

A limited amount of heat-transfer data for the pool heating of liquid hydrogen appears in the literature (cf., refs. 1 to 4). The pool boiling of many fluids other than hydrogen is extensively reported in the literature. Several well-known correlations for predicting pool boiling heat-transfer rates have been profferred (ref. 5). It cannot be assumed a priori that these correlations can be applied to boiling hydrogen.

In the boiling regime, several investigations have been made concerning the effect of gravity on the mechanism of boiling. Siegel and Usiskin (ref. 6) conducted an experiment with water at zero or near-zero gravities. Similar

experiments with hydrogen and nitrogen were reported in references 1, 6, 7, and 8 for the low-gravity condition. Several investigators have studied boiling and burnout in multigravity conditions (refs. 9 to 13), but none of the studies has been with hydrogen.

The object of the experiments reported herein was to assess the effects of multigravity on both the boiling and supercritical heating of liquid hydrogen. Measurements were taken to determine (1) the amount of energy going into the heater, (2) the heater surface temperature at three locations, and (3) the bulk hydrogen temperatures and pressures. High-speed photographs, including shadowgraphs, were taken of the fluid during heating. The high-speed movies were valuable in gaining insight into the mechanism of heat transport. Motion-picture supplement C-224 has been prepared and is available on loan. A request card and a description of the film are included at the back of this report. The effects of heater geometry on the heat-transport mechanism were also assessed.

SYMBOLS

A	area, sq ft
c	heat capacity, Btu/(lb_m)(^oF)
c_p	specific heat, Btu/(lb_m)(^oF)
g	acceleration due to gravity
g_c	constant for converting from force to mass units
h	heat-transfer coefficient, Btu/(sq ft)(hr)(^oF) or Btu/(sq in.)(sec)(^oF)
i	current
K	arbitrary constant
k	thermal conductivity, Btu/(ft)(hr)(^oF)
L	length, ft
M	constant used in ref. 20, 274 ft^{-1}
Nu	Nusselt number
n	number of g's
P	correlation parameter used in ref. 20, hr/Btu
Pr	Prandtl number, $c_p\mu/k$
p	pressure

p_o	pressure of 1 atm
Q	heat rate, Btu/hr or Btu/sec
Q_{gen}	electrical power generated
Q_{ht}	heat transferred
q	heat flux, Btu/(sq ft)(hr) or Btu/(sq in.)(sec)
R	width of heater, ft
r	electrical resistivity, (ohm)(ft)
Ra	Rayleigh number of free convection, $g\beta \Delta T L^3/\alpha\nu$
T	temperature
V	voltage
w	width, ft
x	thickness, ft
α	thermal diffusivity, $k/\rho c_p$, sq ft/hr
β	coefficient of bulk expansion
λ	heat of vaporization, Btu/lb
μ	dynamic viscosity, lb/(ft)(hr)
ν	kinematic viscosity, sq ft/hr
ρ	density, lb_m/cu ft
σ	surface tension, lb_f/ft

Subscripts:

b	bulk
c	critical
i	inner
l	liquid
sat	saturation
v	vapor
w	wall
0	reference

APPARATUS

Overall Apparatus

Figure 1(a) is a sketch of the 4-foot arm centrifuge used to impose the varying multi-g acceleration forces on the fluid. The centrifuge was rotated by an air turbine, and the speed was measured with an electronic frequency counter. The mounting of the tank and high-speed motion-picture camera at the end of the arm is schematically shown in figure 1(a).

The tank and the heating element are shown in figure 1(b). The tank was approximately 2 quarts in volume and was equipped with observation and illumination windows for the photography. The tank was mounted on a free-rotating trunnion arrangement (see fig. 1(a)) that automatically enabled the tank-heater assembly to be oriented so that the resolved acceleration vector (gravitational plus centrifugal) was perpendicular to the heater surface.

The tank was constructed like a Dewar in order to contain the liquid hydrogen. The inner tank, which actually held the hydrogen, was insulated with spaced laminations of aluminum foil. A vacuum was maintained in the void regions between the layers of foil. As shown in figure 1(a), the vacuum pump rotated with the arm to maintain this vacuum. Provision was made for pressurizing the Dewar and controlling this pressure to some preset value. A bleed line and a pressurizing line were required to make this possible. The bleed line was connected to an atmospheric vent that rotated with the apparatus. A strain-gage transducer was used to measure the tank pressure.

Heater

Two heater geometries were employed. Schematic drawings of these are shown in figure 1(c). In one geometry, the heater surface is surrounded by a plastic shield; in the other, it is not. All other features of the heater, such as the heater ribbon geometry and instrumentation, are identical. A part of the investigation was to assess the effect of the shield on the heat-transfer results.

A cross-sectional view of the heater block and its associated surface temperature instrumentation is shown in figure 1(d). The heating element was a thin (0.0060-in. thick) Chromel A ribbon mounted over a Bakelite block. The ribbon was tension-mounted with springs on each end and was cemented to the surface of the Bakelite block. The purpose of the tension mounting was to prevent buckling of the strip when it expanded during heating. By virtue of this mounting, the ribbon heated the fluid from one side only. An alternating-current power source furnished the electrical energy to the ribbon. The cross-sectional area of the ribbon was considered to be very uniform from end to end; thus a uniform heat flux was developed over the entire heater length by resistive heating.

Considerable difficulty was incurred in developing a thermocouple system that would measure the surface temperature of the heater reliably. The hydrogen pool was found to be the optimum location for the cold junction. It is well

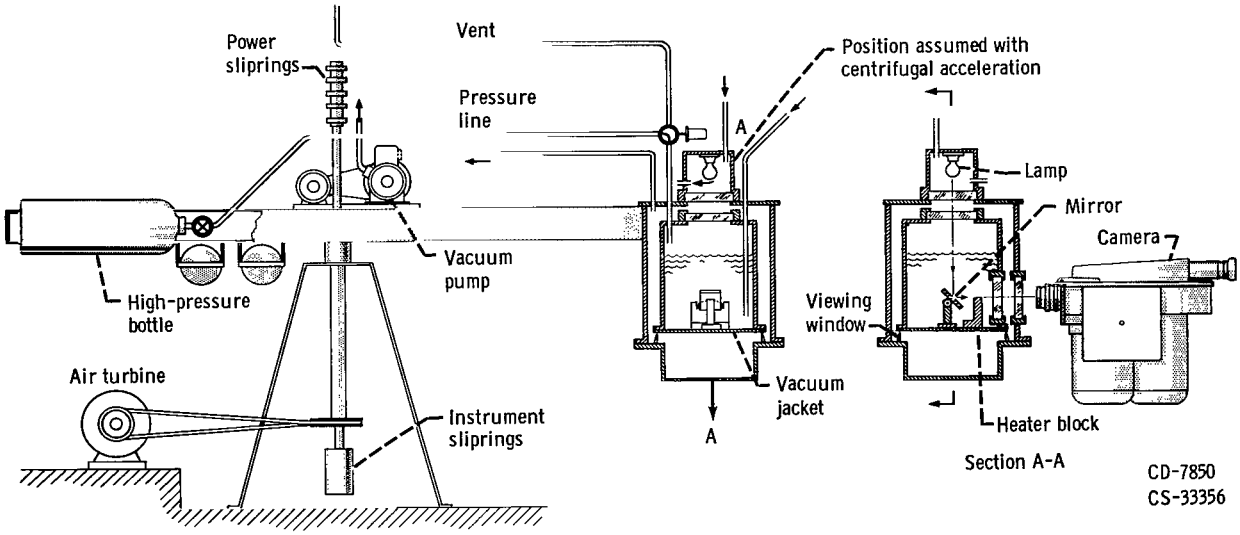

(a) Centrifuge assembly.

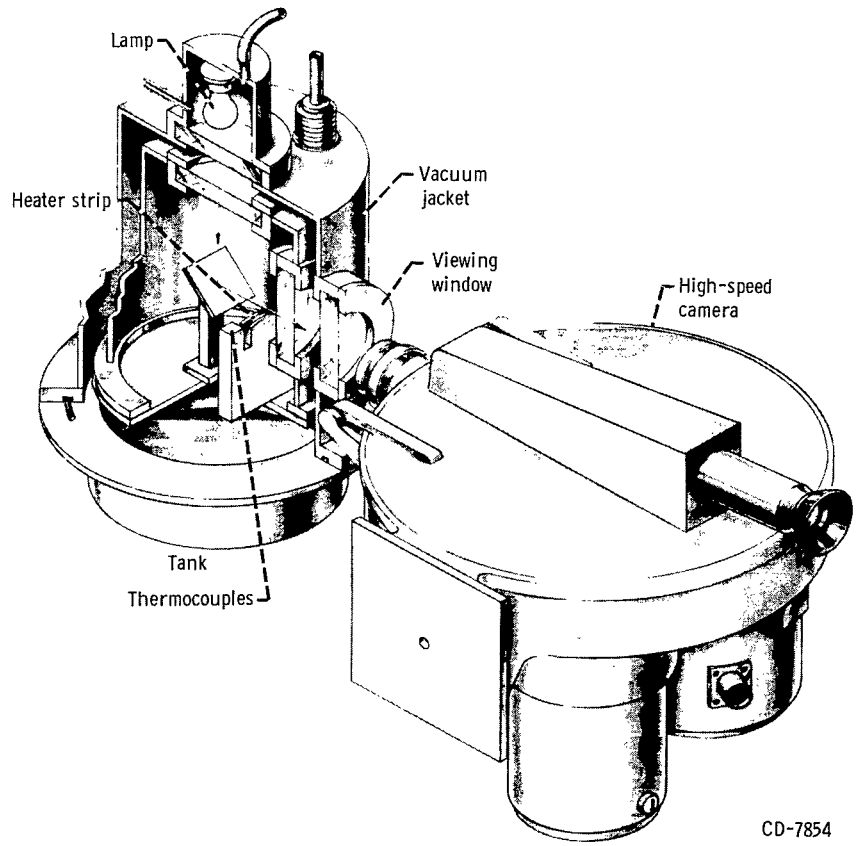

(b) Tank and camera assembly.

Figure 1. - Centrifuge apparatus.

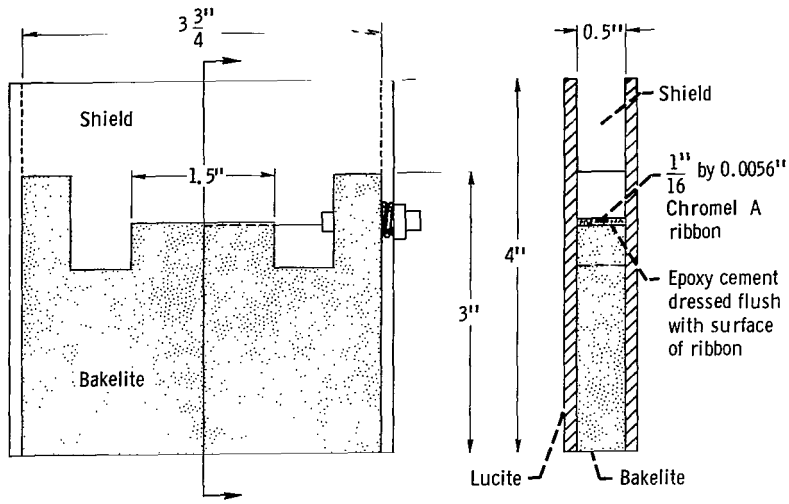

(c) Heater and shield geometries.

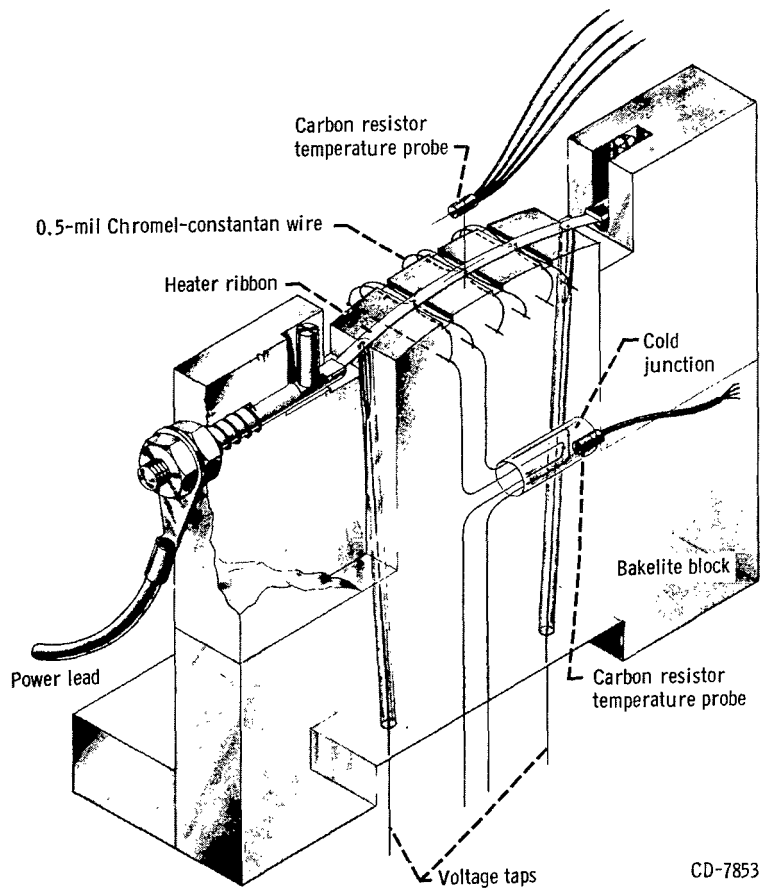

(d) Cross-sectional view of heater block and associated surface temperature instrumentation.

Figure 1. - Concluded. Centrifuge apparatus.

known that the electromotive force output from an ordinary thermocouple decays to a small amount at liquid-hydrogen temperatures. Consequently, it was difficult to measure small differential temperatures between the hydrogen and the heater. It was desired that local surface temperatures be measured, however, and the use of a thermocouple seemed to be the most feasible technique for obtaining the temperature of a very small contact area. Chromel-constantan was chosen as the thermocouple material because it provided approximately 50 percent greater electromotive force output than copper-constantan, and the junction is easy to spot-weld.

As is shown in figure 1(d), the three thermocouples were spotted on the back surface of the heater ribbon; this was done to minimize any surface changes provoked by the couple mountings. A small error in actual surface temperature would be incurred, but this was preferred to any alterations in surface conditions that could affect drastically the boiling characteristics of the surface. To minimize the conduction of heat away from the thermocouple junction through the leads, 1/2-mil-diameter thermocouple wire was used. This small-size wire aggravated the installation problem. The cold junctions of the thermocouple were immersed in the hydrogen pool of the Dewar (see fig. 1(d)). Thus the heater thermocouples indicated a temperature difference between the metal temperature and the hydrogen pool; the pool temperature was measured with two carbon resistance probes. The thermocouple output was then amplified by differential amplifiers isolated from common ground, one-hundred-fold for the nucleate-boiling study and sevenfold for the film-boiling portions.

Before this thermocouple system (thermocouples, cold junctions, and amplifiers) was evolved and adopted, there were many hours of preliminary running to check the system. Some of the early preliminary data did not agree with the limited amount of boiling data in the literature. After a careful step-by-step check of the thermocouple system it was found that stray electromotive forces were being introduced in connectors through the vacuum seal of the Dewar. The connectors linked the so-called hot junction to an external cold junction in a boiling nitrogen bath. By moving the cold junction inside the Dewar, this problem was eliminated and the boiling curves obtained corresponded more closely to those obtained by other investigators. Appendix A contains a comparison of various sources of nucleate-boiling data for hydrogen (refs. 1 to 4). As a further check on temperature measurement, a special heater block was made that was instrumented with a small carbon resistor as well as with thermocouples. The temperature measurements of the two devices were compared and were found to agree closely (within 0.5° R). The carbon resistor, even though more suitable for cryogenic temperature ranges, was considered unsatisfactory for general experimental purposes because of its size.

It was anticipated that the sliprings might introduce some error into the temperature measurements, so tests were run in which the sliprings were bypassed, and these results were compared with spinning and nonspinning runs involving the sliprings. In fact, the entire instrumentation was evaluated in this process to avoid slipring errors. It was found that the sliprings did not introduce errors into the recording system. The remaining instrumentation, not mentioned thus far, included voltage taps and current leads on the heater ribbon for heater electrical power measurement.

Recording Devices

Two recording systems were employed in gathering the data reported herein; one was a digital potentiometer, and the other was an oscillograph. All of the basic measurements, including pressure, temperatures, and electrical energy, were transduced to electrical outputs. During most of the running time, a digital potentiometer was used to record these outputs. The digital potentiometer was capable of recording approximately 18 words per second. The actual recording period for a steady-state point was long enough so that each surface thermocouple output was recorded 20 to 30 times. The tabulated differential temperatures represent an arithmetic average of these data. Some of the runs, however, were recorded on an oscillograph, principally those involving high driving temperatures as encountered in film boiling and heating of supercritical hydrogen.

PRECISION OF MEASUREMENT

Estimating the precision of the data recording is difficult. In a recording system like this, many extraneous errors can be introduced through the complexity of the electronics. For example, such things as electrical grounds of various levels will introduce stray electromotive forces into the data output. Also, as was pointed out in the discussion of the heater thermocouples, the heater surface thermometry is being pushed into a temperature region below the accepted applicability and practice. For instance, it is generally recommended that platinum or carbon resistors be used for temperature measurement in the cryogenic regime. The recording instruments were of high precision; the digital potentiometer is rated as possessing a 1/4-percent error at full scale. Perhaps the most difficult measurement uncertainty to assess was the surface temperature accuracy because of the location of the recording thermocouples underneath the heater ribbon. A simplified conduction analysis of the temperature gradient across the thickness of the ribbon was computed for a range of heat fluxes (see appendix B). For the higher heat fluxes ($q = 0.1$ Btu/(sq in.)(sec)), the correction appears appreciable (about 2° R). Table I contains a data column that incorporates this correction. The analysis considers only the temperature difference attributed to the thermal conductivity of the ribbon. Other effects related to the attachment of the thermocouple, such as conduction losses along the thermocouple wire and the mass of the thermocouple junction with its associated thermal and electrical resistivity, were not considered in the analysis. It is felt that such corrections are second order.

The bulk temperatures and pressures of the saturated hydrogen pool were compared with National Bureau of Standards data for para-hydrogen (ref. 14). For some of these checks both a precision platinum and a carbon resistor probe were used. Some deviation from the NBS data was observed. The error in temperature was approximately $1\frac{1}{2}$ percent (0.5° to 1° R absolute error at 100 lb/sq in. abs). Thermal stratification of the fluid in the tank was observed (see appendix C). The relatively small volume of the tank and the observation windows contributed to an appreciable heat leak. Consequently, the tank did

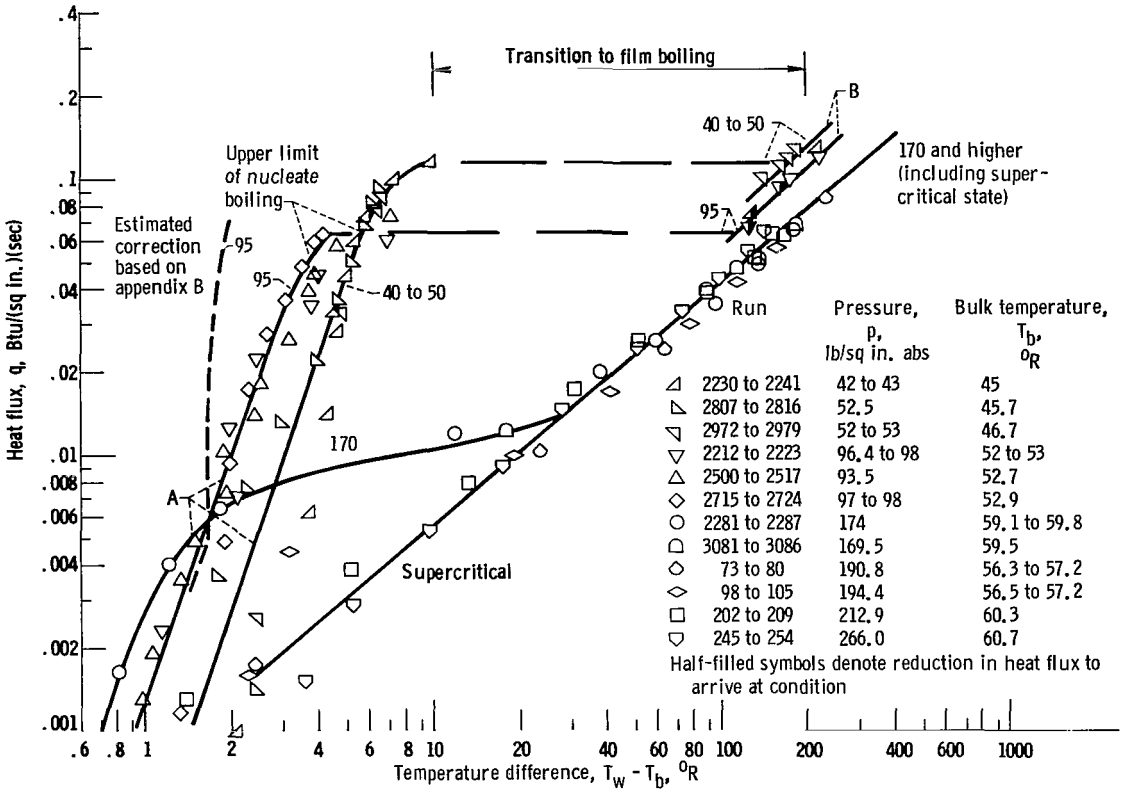

Figure 2. - Heating curve for subcritical (saturated) and supercritical para-hydrogen. Earth gravity.

not provide an equilibrium condition for the measurement of bulk temperature.

Although reproducibility of measurements is not an absolute indication of accuracy, reproduction is necessary for any confidence in the data. For the most part, the data did seem to reproduce quite well even in the difficult nucleate portion of the boiling curve (see fig. 2). It is estimated that the overall accuracy of measurement falls somewhere between 2 and 5 percent. This represents an integrated judgment of the precision of the data-taking system.

PROCEDURE

In general, the procedure was to study first the high-speed motion pictures and heat-transfer data obtained from a heater ribbon in ordinary gravity. Then the multigravity experimentation was programed at thermodynamic conditions comparable to those experienced at 1 g. Generally, a multi-g and a 1-g run were made consecutively for the most meaningful comparison.

As might be surmised, operation of the facility was appreciably more difficult at multi-g conditions than at ordinary gravity. It was much more difficult to hold steady thermodynamic conditions in the Dewar.

Generally, the procedure for getting the multi-g data was identical for the subcritical and supercritical pressure states. The centrifuge rotational

speed was set at a predetermined value, and the heat flux to the heater ribbon was varied over a number of power increments. The experimental conditions covered included the following:

Hydrogen pressure, lb/sq in. abs	60 to 260
Hydrogen temperatures, ^{o}R	45 to 70
Heat flux, q, Btu/(sq in.)(sec)	up to 0.2

The accelerations studied varied from 1 g to approximately 10 g's.

RESULTS

Comparison of Heating Curves for Subcritical and Supercritical States

The multi-g effects can be assessed by comparing multi-g and 1-g data. Unless otherwise specified, all of the local heat-transfer data reported herein are for the center station of the heater block. This selection would tend to eliminate end effects that could influence the two extreme stations.

For the convenience of the reader, the basic data as recorded are presented in table I. Also included in table I are differential temperatures and heat fluxes that are corrected for estimated errors in the measurement of these quantities. (See appendix B for a detailed discussion of the methods of correction.) In some saturation cases, the bulk temperature does not agree with the NBS saturation data. Maximum deviation is approximately 1^{o} R (see the section PRECISION OF MEASUREMENT).

Figure 2 shows the heating curves for hydrogen obtained with the heater block shown in figure 1(c) in both the subcritical- and supercritical-pressure regimes in an Earth gravity environment (gravity vector normal to the heater surface). Only saturated subcritical data are shown. In general, this figure looks quite similar to comparable plots for other fluids such as Freon (ref. 15) and water (ref. 16). There are a number of interesting features in this figure. First, there is a very steep portion of the heating curve (labeled A) associated with various nucleate-boiling mechanisms. The level of the temperature difference ($T_w - T_b$) associated with nucleate boiling is a function of pressure; the ΔT decreases with increasing pressure. Further, there is a film-boiling region (labeled B) that extends over an extensive range of heat fluxes and driving temperatures. In the strictest sense, the "film-boiling region" involves a transition from nucleate to film boiling, and liquid wets a part of the wall over most of the region. No physical burnout of the heater was encountered over the range of conditions presented in figure 2. At the higher driving temperatures, it should be observed that the film-boiling and supercritical data tend to merge into one band. Apparently, the mechanisms for the heat transport are similar for both fluid states. There appears to be a pressure dependency on film boiling. This has been observed with other fluids.

Associated with the development of the boiling curves was an observable hysteresis phenomenon that influenced the data points in transition from

nucleate to film boiling. More will be said about the hysteresis phenomenon in a later paragraph. The hysteresis effect did enable more data to be gathered in the transition region between nucleate and film boiling by extending the film-boiling curves to lower heat fluxes. When the heat flux was being increased during the test procedure, a discontinuous jump from the nucleate- to the film-boiling region took place. This is not to imply that a true discontinuity in the boiling curve exists. The jump occurred because heat flux, instead of wall temperature, was the controlled variable. By gradually decreasing heat flux, data points within the transition gap could be obtained, and several of these appear on this figure as half-filled points.

Returning to a discussion of the nucleate portion of the curve, it is obvious that only a small driving temperature is required for the nucleate boiling of hydrogen. For saturated water, the driving temperature in nucleate boiling is an order of magnitude higher. It is also observed that pressure level, or rather proximity to critical pressure, has a pronounced effect on the nucleate portion of the boiling curve. As the pressure level approaches the critical value (from the low side), the span of heat fluxes associated with the nucleate-boiling curve decreases, until at (or near) critical pressure there is no steep-sloped nucleate curve. Since the heat of vaporization of hydrogen diminishes with increasing pressure, it may be postulated that the enhanced heat-transfer rate in the nucleate regime is related to the evaporation process. Whether evaporation or the stirring action of bubbles controls the enhancement of heat transfer in nucleate boiling is still a debatable issue. These hydrogen data seem to corroborate recent reports (refs. 17 and 18) that emphasize the importance of evaporation.

Effect of Subcooling on Boiling Curve

Although it was difficult to achieve steady-state experimental conditions with subcooling, some subcooling data in Earth gravity were obtained. The maximum subcooling was of the order of 5° R. Nevertheless, this small amount of subcooling sponsored appreciable changes in the nucleate-boiling curve, as is shown in figure 3. Such a shift in the curve toward higher temperature differences would be expected from nucleation theory (cf., ref. 19) or from an examination of the large amount of subcooled boiling data in the literature for other fluids. It can be concluded that the degree of subcooling is very important in controlling the nucleate-boiling process (particularly incipience) in liquid hydrogen.

Hysteresis Phenomenon in Boiling Curve

In general discussion of figure 2, it was mentioned that a hysteresis phenomenon was encountered in generating the overall boiling curve. Figure 4 shows some typical hysteresis curves obtained with saturated hydrogen. The open symbols represent data points taken while the heat flux was being incrementally increased; the half-filled points represent data taken while the heat flux was being incrementally decreased.

In the operation of the test rig, the operator would incrementally change

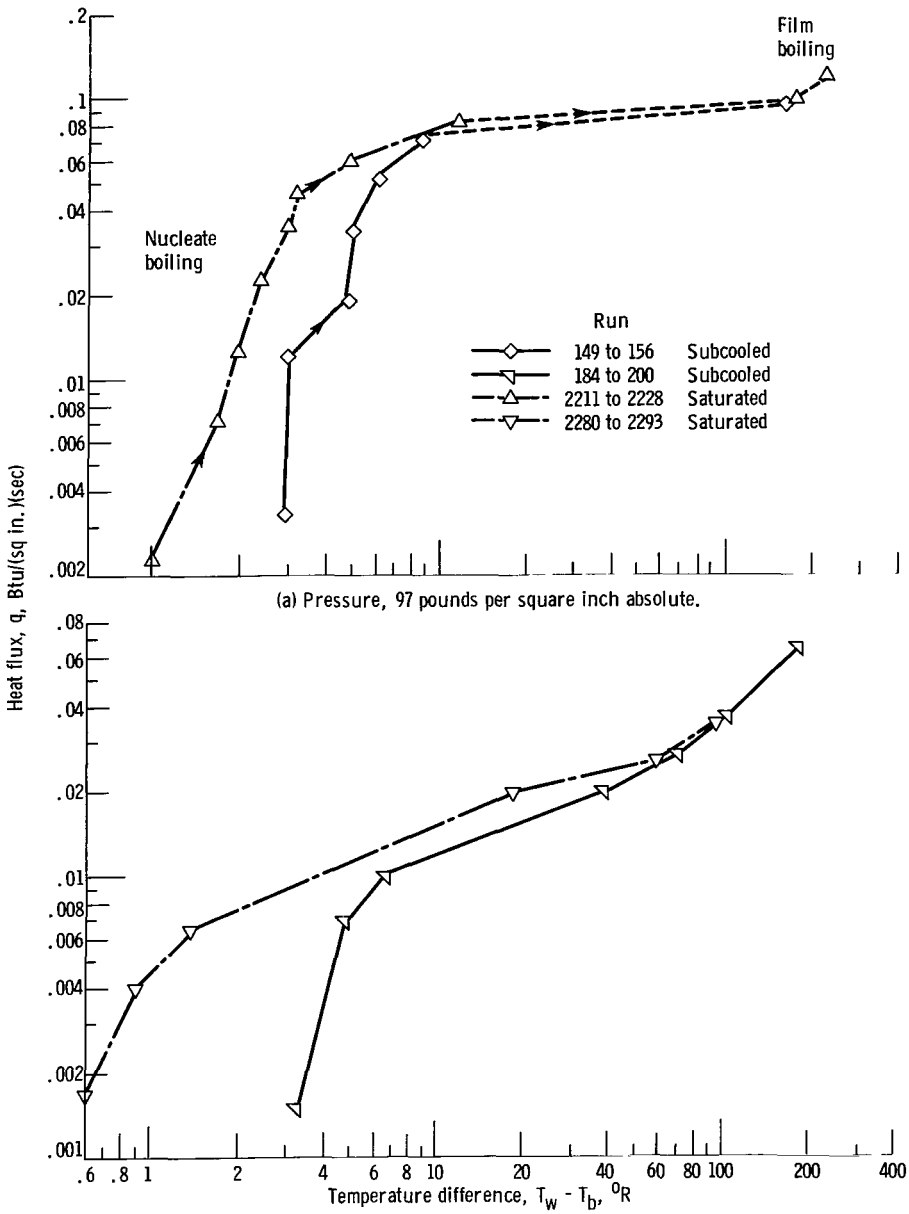

(a) Pressure, 97 pounds per square inch absolute.

(b) Pressure, 175 pounds per square inch absolute.

Figure 3. - Effect of subcooling on boiling curve for para-hydrogen. Earth gravity.

the heat flux. While operating on the nucleate portion of the curve, an upper limit was observed. An increase in heat flux caused sudden transition to the film-boiling portion of the curve. Higher heat-flux points could be obtained in the film-boiling region. Reducing the heat flux would produce another sudden transition back to the nucleate portion of the curve. This lower limit was observed to be approximately equal to or less than the heat flux of the upper limit of nucleate boiling. The arrows in figure 4 indicate the mode of operation during one hysteresis cycle.

As observed in reference 13, the history of the thermal layer has much to

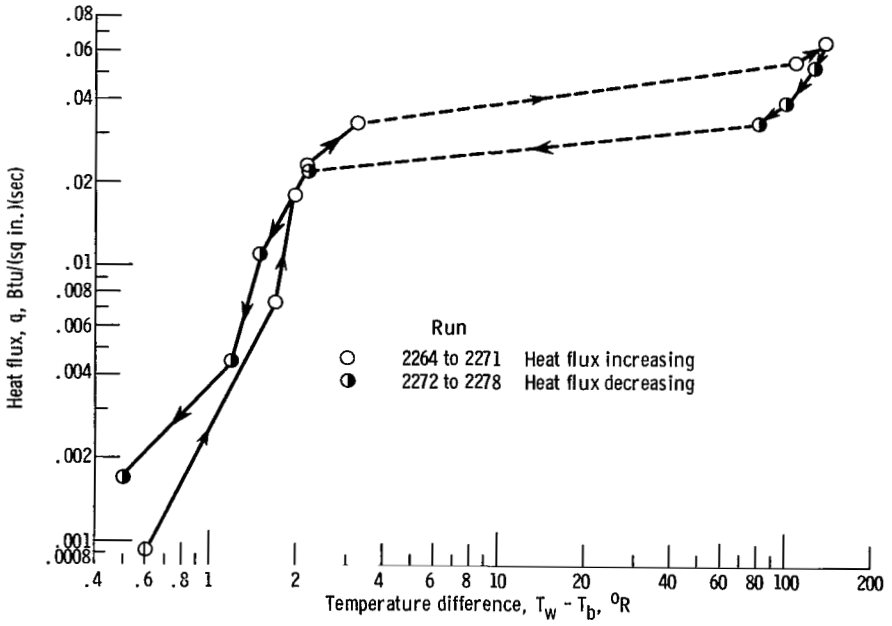

Figure 4. - Hysteresis phenomenon noted in boiling curve for para-hydrogen. Earth gravity.

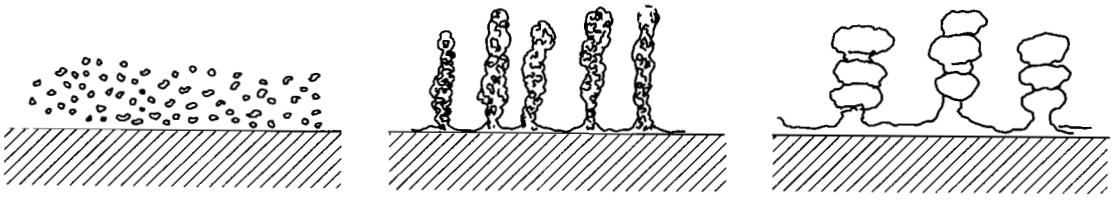

(a) Random, small bubbles; nucleate boiling.

(b) Columnar pattern; nucleate boiling.

(c) Film boiling.

Figure 5. - Patterns of vapor release in nucleate and film boiling of liquid hydrogen.

do with the nature of the boiling curve. Visualization of the boiling process during a hysteresis excursion supported this observation. Figure 5 is a schematic of the bubble or vapor release patterns observed with liquid hydrogen. (High-speed motion pictures showing these are included in the film supplement to this report. Starting with a low heat flux, many small bubble nuclei left the surface (fig. 5(a)). When the heat flux was increased, these small bubbles tended toward a columnar pattern (fig. 5(b)). The columnar pattern became more and more distinct as the heat flux increased. The positions of the columns on the surface did not remain fixed; they tended to oscillate laterally and rapidly over a small area. The end of the nucleate-boiling regime was often heralded by a wisp of vapor that suddenly lifted from the whole surface. Perhaps this wisp of vapor signified the end of any appreciable wetting of the heater surface. Immediately thereafter, a film-boiling phenomenon was observed in which a vapor layer covered most of the surface and large bubbles of vapor rose in a columnar pattern (fig. 5(c)). These film-boiling columns appeared more established than the nucleate variety. There did not seem to be as great a tendency toward lateral oscillation as was observed in the nucleate case. There was a definite reduction in the number of columns as heat flux increased;

along with this, the size of the individual vapor bubbles comprising the columns did increase. It almost seemed as if the increased heating was pushing the columnar pattern to a single column of very large bubbles. In fact, in some preliminary runs, a single vapor chimney was observed.

Decreasing the heating rate from some initial high value showed that film boiling would persist below the heat flux where it started for positive additions of heat-flux increments (see fig. 4). Apparently, the gaseous film would resist the establishment of the wetting film associated with nucleate boiling. This boiling hysteresis possesses similar characteristics to many other physical phenomena such as magnetic induction or flow transition between laminar and turbulent flow. An energy barrier seems to have to be overcome in transitioning between stable states. The transition back to the nucleate columns was not as visually dramatic as the reversed process when a sudden curtain of misty vapor arose. The nucleate-boiling columns could be distinguished from the film-boiling ones by the smaller sized bubbles, the more obvious oscillation of the columns, and the absence of a thick vapor film over the surface.

Multigravity Effects on Nucleate and Film Boiling

Nucleate boiling. - Figures 6(a) and (b) consist of two plots in which 7-g nucleate-boiling data are compared to Earth gravity data at two saturation conditions, pressures of 52 and 90 pounds per square inch absolute. The comparative 1- and 7-g runs were made sequentially, and considerable care was exercised in making the thermodynamic conditions similar. Tank pressure and fluid temperature were carefully monitored before data were taken.

Actually there are three separate heating curves in figures 6(a) and (b), all of which were generated by incrementally increasing the heat flux. The experimental procedure is significant to an interpretation of the comparative data on these plots. First, the Earth-gravity data (curve A) were obtained with a freshly filled Dewar. In the filling procedure, the Dewar was continuously vented to the atmosphere until it would retain a liquid level far above the heater surface. This assured that the inner tank of the Dewar and the heater were in close thermal equilibrium with the hydrogen. Then, the heater surface could be considered to be at liquid-hydrogen temperature. After the 1-g run, the hydrogen Dewar was refilled, the initial thermodynamic conditions of the hydrogen and the heater were reproduced, and the multi-g curve (curve B) was generated. Finally, curve C represents a multi-g repeat that followed immediately after the generation of curve B without a refill. The initial conditions pertaining to curve C were quite different from those of B. The heater was not given adequate time to cool down to the liquid-hydrogen temperature. Also, vapor residue must have been present at the sites. The only certain rapid way of eradicating this residue would have been to refill the Dewar.

A comparison of curves A and B on each plot shows that there is definite movement of the nucleate incipient conditions to a somewhat higher ΔT. These multi-g curves also show a steeper slope of the nucleate curve. As seen in figure 6, curve B generally crosses the 1-g curve and thereafter remains somewhat higher than the 1-g curve.

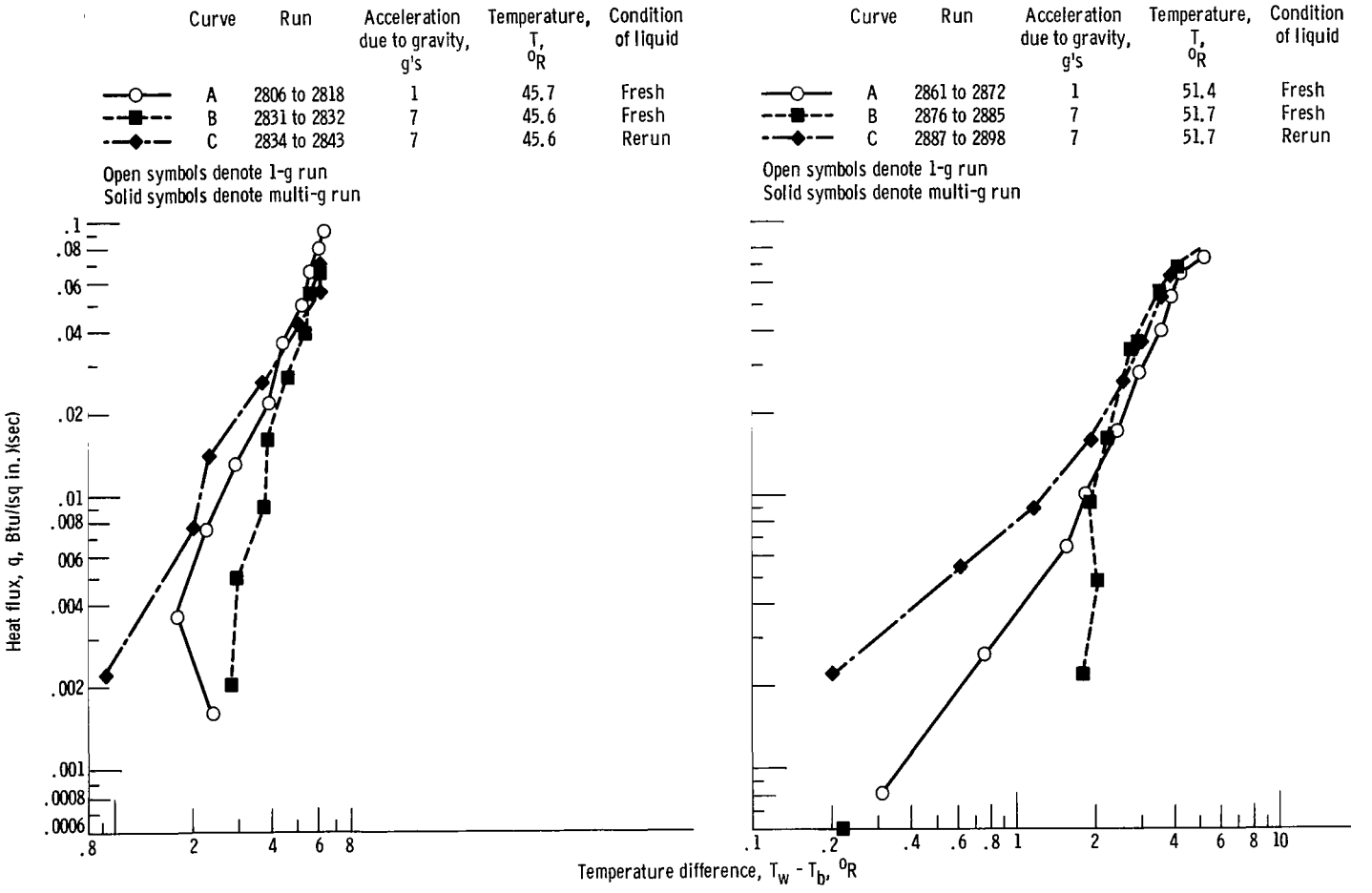

(a) Pressure, 52.4 pounds per square inch absolute; acceleration due to gravity, 1 and 7 g's.

(b) Pressure, 91 pounds per square inch absolute; acceleration due to gravity, 1 and 7 g's.

Figure 6. - Effect of multigravity accelerations on nucleate boiling for saturated para-hydrogen.

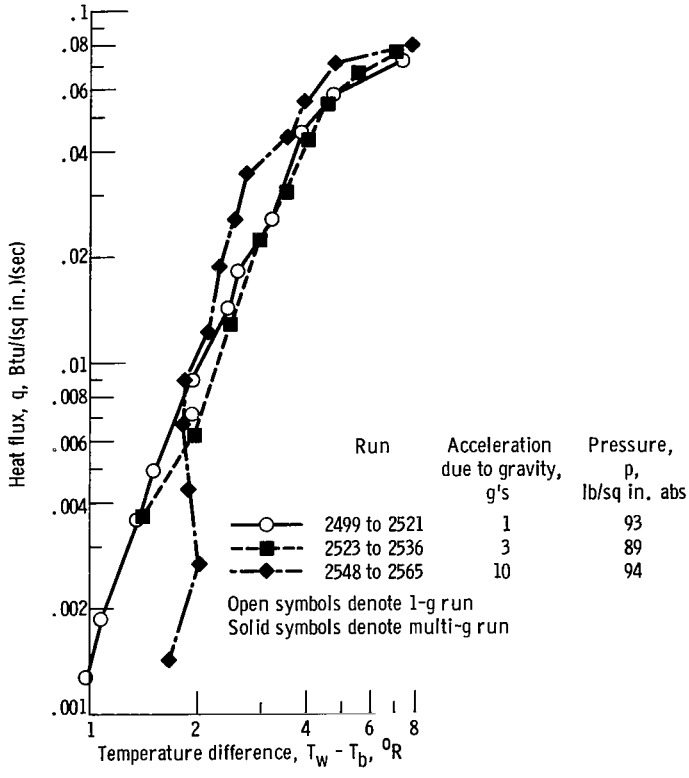

(c) Pressure, 89 to 94 pounds per square inch absolute; acceleration due to gravity, 1, 3, and 10 g's.

Figure 6. - Concluded. Effect of multigravity accelerations on nucleate boiling for saturated para-hydrogen.

An immediate repetition of the multi-g curve leads to a different curve, particularly at the low heat flux and where incipience occurs. Perhaps this can be explained by arguments similar to those profferred in the hysteresis discussion, in which it was pointed out that the history of the thermal layer influences the boiling mechanism. It should be noted that curve B was generated with a newly loaded Dewar of hydrogen. No previous thermal heating of the boundary layer had occurred; thus, the boiling data represent conditions with a virgin thermal layer. In contrast, curve C followed immediately after curve B, with vapor nuclei still residing on the surface. Thus it did not take much driving temperature to initiate nucleation. It is interesting to observe that curves B and C become essentially one curve at the higher heat fluxes.

It can be concluded from figure 6 that a multi-g environment can shift the incipient point of nucleate boiling, but once the boiling has been established, the body force environment does not greatly affect the boiling curve. (There is little spread in the temperature difference for both Earth gravity and multigravities.) This has been confirmed in figure 6(c), which includes 3- and 10-g data. Each curve was generated with a fresh fill of hydrogen.

It has also been learned that the boundary-layer history also markedly influences the boiling curve in the vicinity of the incipient point. Thus it may be concluded from these data that the history and initial condition of the thermal layer are at least as significant as the body force effect in controlling nucleate-boiling incipience. This observation is consonant with what has been observed for subcooling and the hysteresis phenomenon effects.

It should also be noted from figure 6(c) that the upper end of the nucleate curve shows some tendency to move to higher heat-flux values at multigravities. This can be interpreted as an indication that free convection is becoming important in this region of the boiling curve.

Film boiling. - A much more definite body force effect on film boiling was noted that persisted over the entire range of film-boiling conditions investi-

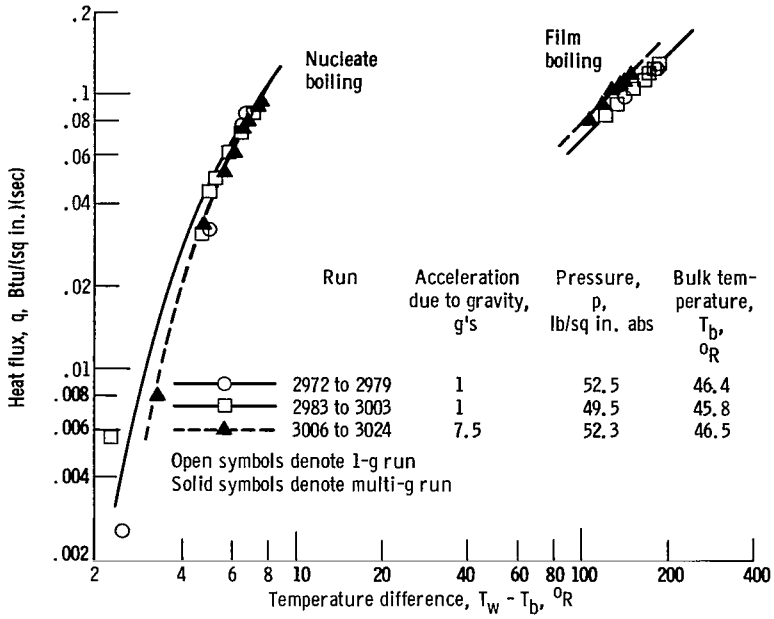

Figure 7. - Effect of acceleration on curves for film and nucleate boiling of saturated para-hydrogen.

gated. Figure 7 shows a comparison of 1- and 7.5-g data in the film-boiling region. The associated nucleate data are shown for comparative purposes. A comparison of the heat fluxes for a given ΔT shows that the 7.5-g data are consistently about 12 to 15 percent above the 1-g data. In obtaining these data, both increasing and decreasing heat-flux experimental procedures were used. Regardless of which procedure was used, the data are reproducible.

Figure 7 does aid in generalizing the effects of multigravity on the nucleate- and film-boiling curves. Figure 7 indicates that there is little gravitational effect on the established portion of the nucleate curve, whereas a definite g-effect is noted in separating the data in the film-boiling portion of figure 7.

Comparison of Hydrogen Data With Nucleate-Boiling Correlations

The heat-transfer data for nucleate-boiling hydrogen at two pressures were compared with two correlations developed for noncryogenic fluids; figure 8 is a comparison of the hydrogen nucleate-boiling data with the correlations of references 20 and 21. For each of these correlations, the hydrogen temperature difference ($T_w - T_b$) is larger than that predicted by the correlations. Appendix D shows how each of these correlations can be reduced to a simplified form, $q = K(\Delta T)^3$ where K is an arbitrary constant. The experimental data (corrected for the conduction temperature difference) indicate that the exponent of ΔT is greater than the predicted values. In addition, the change in the position of the nucleate curve (curve A, fig. 2) with saturation pressure follows a trend indicated by both of these correlations (refs. 20 and 21).

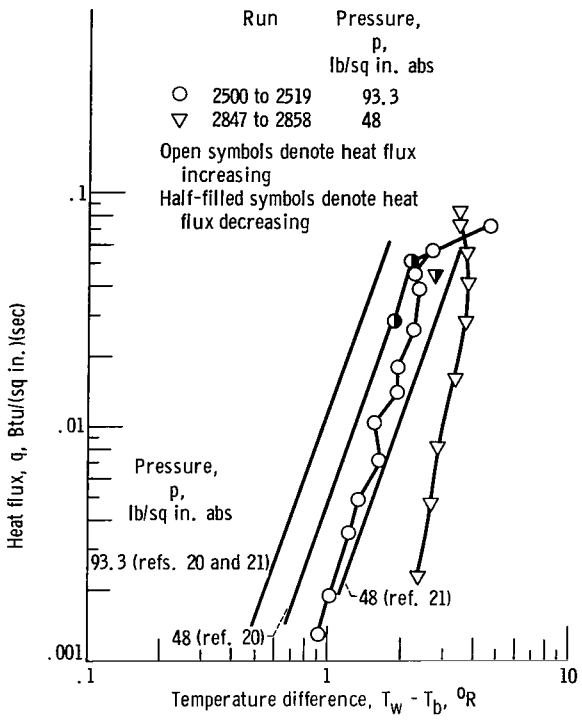

Figure 8. - Comparison of nucleate boiling correlations from references 20 and 21 with hydrogen nucleate boiling data at 48 and 93.3 pounds per square inch absolute. (Coefficient for correlation of ref. 20 adjusted so that predicted values agree with ref. 21 at 93.3 lb/sq in. abs.)

No particular significance can be attached to the degree of departure between the data and the correlations except to point out that, in general, such correlations cannot be expected to apply universally to boiling data. As correlations, they are convenient means for grouping a set (or sets) of experimental data. They also assist in pointing out the influence of parameters or parametric groupings that help in describing physical phenomenon. Thus the applicability of a correlation is also related to the proper selection of significant parameters based on a fundamental understanding of the physics of the process.

Both of these correlations represent efforts to develop dimensionless parameter groupings that are descriptive of the nucleate-boiling process. Both base their models on similitudes between nucleate boiling and convection, and thus construct the familiar convection terms of Reynolds number and Nusselt number pertinent to boiling. For example, in reference 21 the artificial Reynolds number is based upon the velocity of vapor-liquid exchange in the ebullition process, and the characteristic dimension is a computed maximum bubble size. In the correlation of reference 20, dimensionless groups are developed that are based upon "a stirring length of the bubbles," the velocity of the bubbles, and the number of bubbles developed per unit of time. These can be construed to be elements of a convection-like mechanism caused by the action of bubbles.

The discrepancy between the hydrogen data and these two nucleate-boiling correlations may be explained by a number of possibilities. First, these correlations do contain empiricisms that are based on other fluids and different heater geometries. It has been demonstrated throughout the boiling literature that heater geometry, surface conditions, and the nature of the fluid affect the heat transfer results. Both references 20 and 21 have inserted empirical constants in the correlations to account for these effects. By changes in the empirical constants the hydrogen data could be fitted with correlation equations similar to those presented in the references. In fact, the value of the parameter P in the correlation of reference 20 was based upon experimental observations made by the originators of the correlation. In reference 20, it is made clear that the numerical value of P is dependent on the fluid, the surface conditions, and the heater geometry. Thus, it would appear difficult to apply this correlation a priori to any boiling fluid or heater geometry. An experimental program would be required to determine P, and this

constant could be applied to limited extrapolations of the data. A numerical estimate of P for these hydrogen data will not be made herein because of its doubtful general usefulness in application to other similar heat-transfer situations. Also, the pseudoconvection model applied in obtaining the significant terms of the correlations can be questioned as a proper nucleate-boiling model. For one thing, both correlations would predict an appreciable effect of g on boiling. The term g is explicitly found in the correlation of reference 21, and the heat-transfer coefficient would vary directly with $g^{1/6}$. The gravitational term is not found explicitly in the correlation of reference 20; however, the g-term is implicitly involved in the parameter P, which has been mentioned as an empiricism. The nucleate-boiling hydrogen data reported herein show no appreciable effect of g except for the incipient condition and at the upper limit of nucleate boiling. The credulity of the convection models suggested in references 20 and 21 must be questioned when no experimental gravitational dependence is noted.

A second argument refers to a previous discussion of figure 2. The apparent dependence of established nucleate-boiling hydrogen data reported herein on the magnitude of the heat of vaporization (pressure dependence) is strong evidence of a surface evaporation mechanism as a significant control in the heat-transfer mechanism. This is not to infer that the circulation of the liquid phase near the heater surface does not contribute to the overall heat transfer. But it appears to have secondary importance to an evaporation mechanism over much of the nucleate-boiling regime.

Comparison of Experimental Data With Predictions of Upper Limit of Nucleate Boiling

A number of researchers have come up with equations for predicting the upper limit of nucleate boiling. Several of the equations (those by Kutateladze, Zuber, and Wallis) reduce to a similar form. As is pointed out in reference 22, the equation represents the condition where the Helmholtz-Taylor instability upsets the nucleate mechanism. A general form of the equation for the heat flux with Zuber's constant is

$$q = \frac{\pi}{24} \sqrt{\rho_v}\, \lambda [\sigma g g_c (\rho_l - \rho_v)]^{1/4} \qquad (1)$$

Figure 9 shows a comparison of the experimental data for hydrogen with the prediction of equation (1). The experimental values were chosen where the slope of the heat flux against ΔT curve changed radically (see fig. 2). This is the same as saying the heat-transfer coefficient maximizes at these loci.

Note that the predicted curve is relatively insensitive to pressure over a broad range, whereas the experimental points are strongly dependent on it. The predicted value is close to the experimental only in the vicinity of 90 pounds per square inch absolute. For hydrogen, and all fluids in fact, the heat of evaporation decreases rapidly as the critical pressure is approached. From figure 9, it is obvious that the experimental curve diminishes more

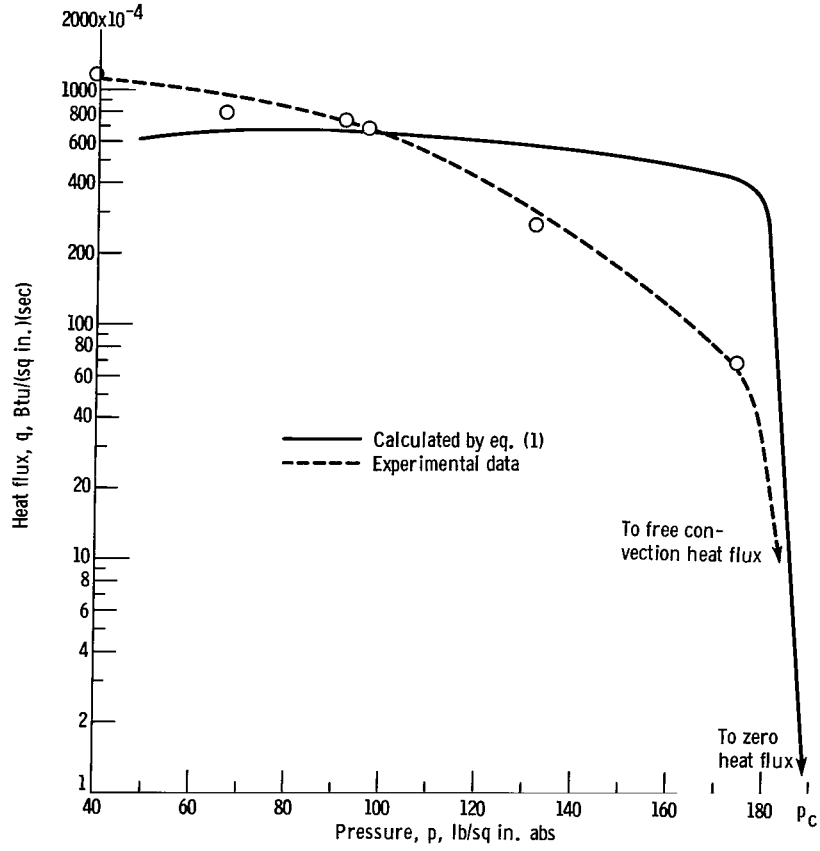

Figure 9. - Comparison of upper limit of nucleate boiling with prediction of reference 2 for saturated para-hydrogen. Earth gravity.

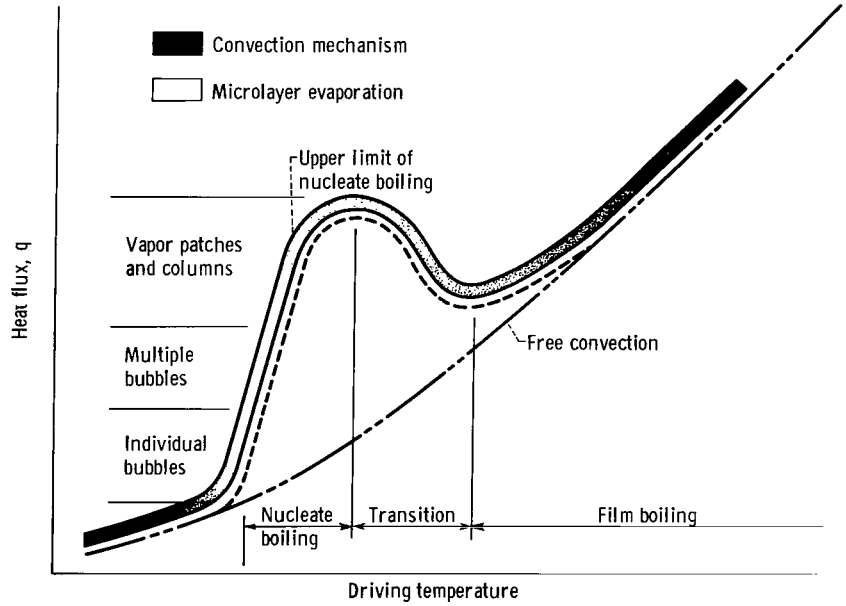

Figure 10. - Schematic of mechanisms associated with boiling.

rapidly than the predicted one as critical pressure is approached.

Reference 22 contains an extensive discussion on the upper limit of nucleate boiling and the nucleate-boiling mechanism that lead up to this limiting condition. At the low heat-flux end of the nucleate-boiling curve, there is the region of isolated bubbles where bubble "up-draughts" and liquid circulation account for the heat transfer; the regime can be treated as a free convection problem. At higher heat fluxes, there is a region of vapor columns and patches where vaporization is the principal transport mechanism. The upper limit of nucleate boiling is marked by a Taylor-Helmholz instability. Thus, the upper limit is in a domain where the evaporation is predominant.

The authors of this report would suggest a somewhat different interpretation of the upper limit of nucleate boiling and the progression of events that would lead to this condition as heat flux is increased. Figure 10 is inserted to aid in presenting this interpretation. Starting at the low end of the heating curve, it is obvious that a free convection mechanism establishes this portion of the curve. At some higher heat flux and ΔT, boiling first makes its appearance through the development of a limited number of individual bubbles. Perhaps only one or two sites are active. Free convection does influence the incipient point (see section on Multi-g effects on nucleate boiling). An incremental addition of heat could contribute to the inception of many sites. Once boiling was established, the heating curve would depart radically from the convective slope. The initial departure could be ascribed to an evaporative component (ref. 18) and an enhanced free convection associated with rising bubbles.

Judging from the results shown in references 17 and 18, it is felt that the evaporative contribution becomes predominant after the transition into the boiling curve has been completed. Thus a surface phenomenon involving the evaporation of a liquid film microlayer in the vicinity of the sites appears to be a dominant influence that improves the heat transfer beyond the free convection level. The presence of this microlayer for a wetting fluid has been definitely established (ref. 23).

In the patch and vapor column regimes of nucleate boiling, it becomes increasingly difficult for the evaporative microlayer to be maintained. A Taylor instability involving the liquid and vapor streams begins. The heat transport begins to be influenced by a free-convection-like mechanism involving the two phases that takes place adjacent to the wall. The upper limit of nucleate boiling marks the loci where heat of vaporization begins to lose its dominating role in the heat transfer. It is appropriately named. An incremental increase in heat flux beyond this upper limit brings about a film-boiling condition with an entirely different dominating mechanism.

Much of this argument is based upon the multi-g observations contained herein, which showed that most of the established portion of the nucleate-boiling curve was insensitive to multi-g level. If bubble stirring and liquid circulation (free convection mechanisms) were of prime import, the heat-transfer data would depend on g. A definite g-dependence was noted in the film-boiling region. In fact, a power on the Rayleigh number Ra would predict the change in the film-boiling heat flux in going from 1-g to the multi-g

condition. Thus, a free convection mechanism in the gas layer adjacent to wall seems to dominate in this region. A further point of argument will be presented in the section Supercritical Heating.

Supercritical Heating

It has been noted already from figure 2 that the supercritical heating data fall along a fairly linear band (on a log-log plot of q against ΔT). This is similar to what would be observed for the free convection of any fluid. The slope of this hydrogen data, however, is less than that which is generally predicted for ordinary gases; the slope for gases is approximately 1.2, and for these hydrogen data it is 0.9. No conclusive explanation for this difference can be offered. No hysteresis or apparent dependence on experimental procedural technique was encountered in getting data that would group within a narrow band.

Visual studies of the supercritical regime showed that a phenomenon somewhat resembling columnar boiling (see fig. 5(c)) was at work. Of course bubbles were not present, but sizable low-density agglomerates were rising through a denser and colder fluid. This gave the appearance of boiling to the heating process. The motion of these agglomerates is readily observed in selected film clips that are part of the film supplement to this report.

This boiling-like mechanism for a supercritical fluid is shown in the high-speed photographs of Freon in reference 15. Also, the possibility of such a mechanism was postulated in a prepared discussion by Goldmann to reference 24. The mechanism was postulated to explain the enhanced heat transfer near the critical point.

The observation of a boiling-like mechanism in the supercritical state adds another argument to the boiling mechanism discussion of the previous section. In the film supplement, the fluid appears to be as agitated in the supercritical regime as it is in the subcritical. Yet this supercritical agitation produces heat-transfer coefficients that are not nearly as large as those observed in nucleate boiling (see fig. 2). It follows then that agitation cannot be the sole source of the enhanced nucleate-boiling heat-transfer coefficient. Another component, namely evaporation, must be significantly influential. Examination of figure 10 reveals that the supercritical domain can be represented by the free convection band. This band depicts the similitudes in the heat-transfer mechanisms between the supercritical and subcritical pressure states. Such similitudes occur in the nonboiling free convection and film-boiling regions identified in figure 10.

Multigravity Effects on Supercritical Heating

Figure 11 is a comparison of 1- and 7-g heat-transfer data for supercritical pressures. The data include two pressures, 215 and 260 pounds per square inch absolute. Regardless of the pressure level, the data group into two distinct band, Earth gravity and multigravity; multi-g data fall above the

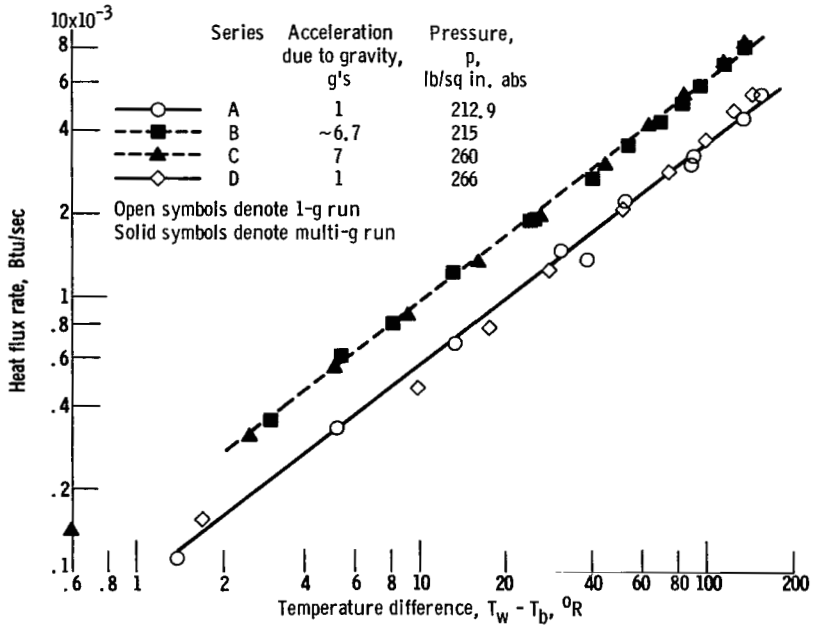

Figure 11. - Effect of multigravity accelerations on supercritical heating for para-hydrogen.

1-g data. If some sort of free convection correlation involving a Rayleigh number were assumed, this trend would be expected. Furthermore, in free convection correlations, the exponent on the Rayleigh number may range anywhere from approximately 0.25 to 0.35. Consequently, the ratio of the multi-g heat flux to the Earth-gravity heat flux should be

$$\frac{q_{ng}}{q_{1g}} = (n)^{0.25 \text{ to } 0.35} \tag{2}$$

where n is the number of g's imposed. The ratio of the g's from figure 11 appears to be about 1.65; thus the exponent of n would be approximately 0.26. This is within the range of values cited for free convection. Thus, it may be concluded that the supercritical heating of hydrogen in multigravity may be predicted from a standard free convection correlation using 1-g data as a reference situation.

Effect of Shield Geometry on Heat Transfer

A part of the investigation was to assess the effect of a chimney-like shield on the heat-transfer results (see fig. 1(c)).

Figure 12(a) presents the data for nucleate and film boiling at two subcritical pressure levels around 90 and 170 pounds per square inch absolute for the two geometries. Both 1- and 7-g data are included. There appears to be no discernible shield effect for this particular geometry within the small

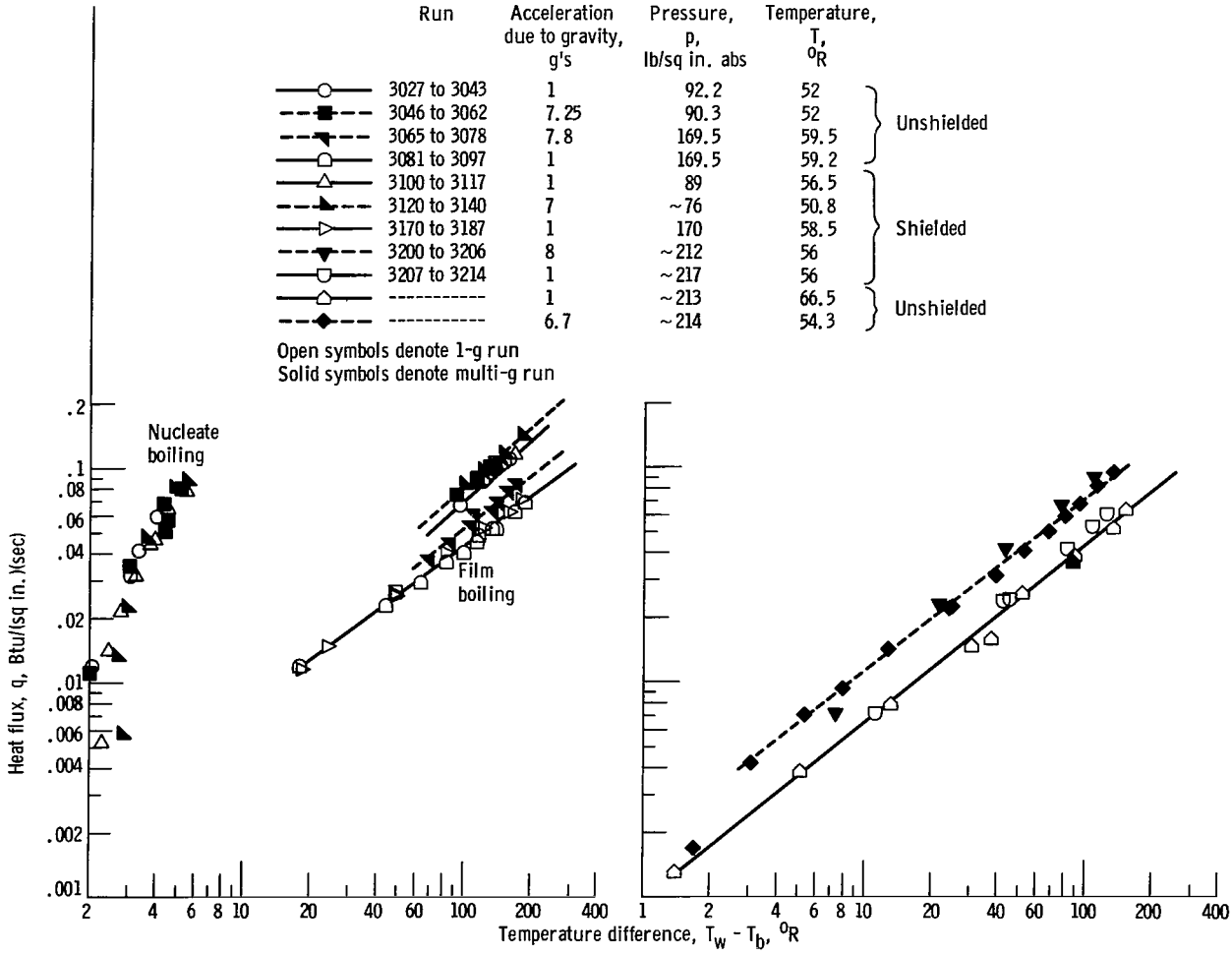

(a) Nucleate and film boiling of para-hydrogen.

(b) Supercritical heating of para-hydrogen.

Figure 12. - Effect of shielding on heating curve for 1-g and multi-g conditions.

scatter of the data. It is to be noted that the same gravitational effects were observed with the shielded geometry as with the unshielded. A tendency toward higher heat fluxes for the shielded geometry in the film-boiling region might possibly be observed.

The supercritical pressure data taken at 1 g are shown in figure 12(b). Comparison of the two geometries shows a slight tendency of the shielded data to fall above the unshielded. The shield tends to encourage circulation patterns that improve the natural convection heat transfer. If the cross-sectional size of the chimney were reduced, the shield effect would probably be more pronounced. Similar effects were shown by comparison of the multi-g data.

CONCLUSIONS

As a result of this investigation, which involved a horizontal ribbon-type heater tested at hydrogen pressures of 60 to 260 pounds per square inch absolute, hydrogen temperatures of 45° to 70° R, heat fluxes of up to 0.2 Btu per square inch per second, and accelerations of 1 to 10 g's; the following observations or conclusions are made:

1. The heating curves (heat flux against temperature potential) for liquid hydrogen in the subcritical and supercritical pressure states are similar to curves for other fluids. In the subcritical state, nucleate- and film-boiling regions are clearly indicated. The upper limit of the nucleate curve is pressure dependent. The film-boiling and supercritical heating curves tend toward coincidence at high heat fluxes.

2. The nucleate portion of the subcritical heating curve is sensitive to subcooling and hysteresis effects. With the exception of bubble incipience, very little influence of multigravity effects on temperature difference was noted on the curve. There probably is some tendency for the upper limit of nucleate-boiling heat flux to shift upward as the acceleration due to gravity is increased. The presence of a chimney-like shield did not affect the heating curve. Existing nucleate-boiling correlations of Nishikawa and Rohsenow do not serve as accurate means for predicting the heating curve a priori. Once a heating level has been established experimentally, these correlations can be fitted with constants and used for extrapolative predictions. Also, the analytical predictions for the upper limit of nucleate boiling used successfully with water do not work with hydrogen. They do not reflect the severity of the pressure dependence noted in the experimental results.

3. No hysteresis effects were noted in the established film-boiling region of the boiling curve; however, a definite hysteresis phenomenon was noted in the transition region between nucleate and film boiling. In fact, certain operating points could only be achieved by approaching from a high heat flux to a low one. In the established film-boiling region, a change from 1 to 7.5 g's produced a 12- to 15-percent increase in the heat flux.

4. As a result of these experimental observations with hydrogen, it does seem evident that these nucleate-boiling data support the liquid microlayer model discussed by Moore and Messler and in TN D-2290. Admittedly, the nucleate-boiling mechanism is a complex mixture of submechanisms that involves both bubble dynamics and surface evaporation. Such factors as bubble population, frequency, and the geometry of the bubbles (single or multiple) undoubtedly influence the overall mechanism. The fact that the nucleate data are insensitive to g-level and heater shielding but are sensitive to thermal layer history (hysteresis) and subcooling is taken as evidence that the nucleate mechanism is primarily a surface phenomenon and does not depend on such things as free convection of the pool or the stirring action of bubbles.

The boiling-like agitation noted in the supercritical pressure regime did not produce as high a heat-transfer coefficient as was experienced in nucleate boiling. This is interpreted as a further indication that the primary influence in the enhanced heat transfer of established nucleate boiling cannot be bubble stirring.

5. It is suggested for further investigation that the upper limit of nucleate boiling represents the end of the controlling regime of the evaporative microlayer mechanism. Beyond this point, free convection forces within the vapor layer adjacent to the wall become controlling in the transition to the film-boiling region. At the upper end of the film region, there is little

contribution by the heat of vaporization. This free convection model is supported by observations of enhanced heat transfer in the established film-boiling region when the gravity level was increased.

6. It is also concluded that the mechanisms of heat transport for established film boiling and supercritical heating are similar. The high-speed photographic evidence (see film supplement) and the heat-transfer data support this conclusion. This similarity also supports the view that free convection is the primary mechanism in the film-boiling region. The gravitational dependence of the supercritical data followed the Rayleigh number (free convection) prediction, but the slope of the heating curve was less than the slope for the free convection of gases on horizontal surfaces.

Lewis Research Center
National Aeronautics and Space Administration
Cleveland, Ohio, November 9, 1964

APPENDIX A

LIMITED COMPARISON OF HYDROGEN NUCLEATE-BOILING DATA WITH LITERATURE VALUES

Some of the nucleate data reported herein were compared with hydrogen boiling data in the literature (refs. 1 and 2). No direct comparisons can be made because of differences in the heater geometries and probable differences in the surface conditions for the experiments cited. Nevertheless, figure 13 shows that there is relative agreement among the data for the ΔT level, the slopes of the boiling curves, and the pressure effect on the boiling curves. This agreement adds to a confidence in the surface temperature measurement.

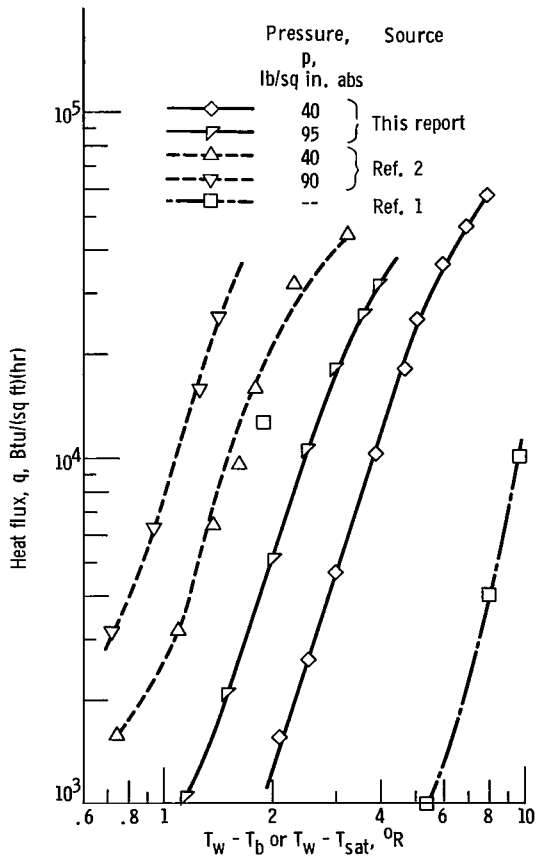

Figure 13. - Comparison of nucleate boiling data with several literature sources.

APPENDIX B

ANALYSIS OF TEMPERATURE DIFFERENCE ACROSS THICKNESS OF HEATER RIBBON

As an approximate analysis of the temperature gradient across the thickness of the heater ribbon, the following assumptions were made:

(1) The electrical power generation in the strip was uniform in all directions at any given axial location.

(2) The gradient in voltage drop along the length of the heater is constant.

(3) Such properties of the material as thermal conductivity k and electrical resistivity r are isotropic and are assumed to be constant across the thickness of the heater element (the temperature differences are small).

(4) The heat generated within the element flows in one direction, toward the liquid interface (see fig. 14).

Using the terminology of figure 14 and considering the thermal balance at an element (denoted by the dashed lines) result in the following:

$$Q_{gen} = Q_{ht} \tag{B1}$$

The electrical power generated Q_{gen} is

$$Q_{gen} = \frac{\Delta V^2}{\frac{r\ \Delta L}{\Delta x\ w}} \tag{B2}$$

The heat transferred to the liquid is

$$Q_{ht} = w\ \Delta L\ \frac{dq}{dx}\ \Delta x \tag{B3}$$

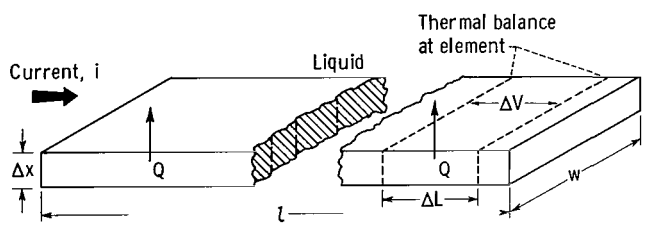

Figure 14. - Model of heater ribbon employed in conduction analysis of appendix B.

Thus, equation (B1) becomes

$$\frac{dq}{dx} = \frac{1}{r}\left(\frac{\Delta V}{\Delta L}\right)^2 \tag{B4a}$$

Since it is assumed that the voltage gradient is constant and r is independent of x,

$$\left.\begin{aligned} \frac{dq}{dx} &= C_1 \\ \text{or, by integrating,} \qquad & \\ q &= C_1 x + C_2 \end{aligned}\right\} \tag{B4b}$$

Since the boundary conditions specify that the heat flux is zero at $x = 0$, the constant C_2 will be zero. Since

$$q = -k \frac{dT}{dx}$$

equation (B4b) can be integrated across the thickness of the strip to solve for the temperature differential between the inner and outer surfaces; that is,

$$-k \int_{T_i}^{T_w} dT = \frac{1}{r} \left(\frac{\Delta V}{\Delta L}\right)^2 \int_0^{x_0} x \, dx \tag{B4c}$$

or

$$k(T_i - T_w) = \frac{1}{r} \left(\frac{\Delta V}{\Delta L}\right)^2 \frac{x_0^2}{2}$$

Simplifying this equation results in

$$T_i - T_w = \frac{Q_{gen} x_0}{2k} \tag{B4d}$$

There are no thermal conductivity data for annealed Chromel A in the cryogenic temperature range in the literature. The only similar material for which cryogenic thermal conductivity data are available is Inconel. The conductivity data were obtained from reference 25. The Inconel information at a mean temperature of approximately 48° R is used to determine the temperature difference between the surfaces of the ribbon for various heat fluxes, which is shown in the following table:

Heat flux, q, Btu/(sq in.)(sec)	Temperature difference, ΔT
0.001	0.022
.01	.22
.1	2.24

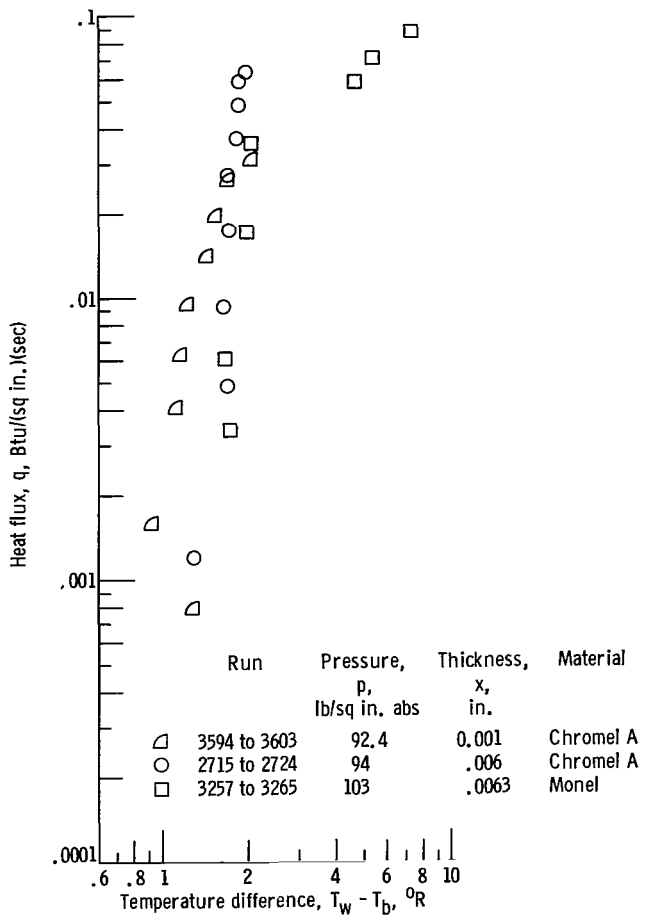

Figure 15. - Comparison of corrected wall temperatures of various heater thicknesses and materials. Temperature, 51° R.

A series of tests in which the thickness and material of the heater was varied give a measure of confidence to the estimated values of temperature differences in table I. Heaters were constructed from monel (for which cryogenic conductivities are known) and from thinner Chromel A ribbons. Figure 15 shows the relative agreement for corrected nucleate-boiling data temperature differences among the following heaters:

(1) 0.0060-Inch-thick Chromel A (the heater used throughout the investigation)

(2) 0.001-Inch-thick Chromel A

(3) 0.0063-Inch-thick monel

These data were taken at a mean pressure of 95 pounds per square inch absolute. Thus, they correspond to the estimated correction curve shown in figure 2 and substantiated its general accuracy.

Thus, the maximum error in the measurement of the surface temperature adjacent to the liquid for the range of conditions studied would be of the order of 2° F. The temperature data in table I have been corrected for this conduction effect.

APPENDIX C

STRATIFICATION OF FLUID TEMPERATURE WITHIN THE DEWAR

The proper evaluation of the precision of the hydrogen bulk temperature measurement necessitated an investigation of the local bulk temperature distribution throughout the Dewar volume. The comparatively large surface to volume ratio of the Dewar together with the presence of illumination and visualization windows and instrumentation leads contributed to a substantial heat leak in the tank.

The differential in bulk temperatures at various locations in the tank were checked with both carbon resistor thermometers and Chromel-constantan thermocouples. A maximum of approximately 1° variation in bulk temperature was noted.

APPENDIX D

ANALYSIS OF NUCLEATE-BOILING CORRELATIONS

The correlations of references 20 and 21 predict the proper slopes but not levels for hydrogen nucleate boiling. The equations will be examined to see how the agreement in slope evolves and to determine the sensitivity of the correlations to property variations. The latter may help explain the differences in levels.

By considering the correlation of reference 21 first, the equation is

$$\frac{h}{k_l} Pr_l \sqrt{\frac{\sigma}{g(\rho_l - \rho_v)}} = C_1 \left[\frac{q}{\mu_l \lambda} \sqrt{\frac{\sigma}{g(\rho_l - \rho_v)}} \right]^{2/3} \tag{D1}$$

Regrouping the terms, reducing the exponents, and substituting $h = q/\Delta T$ in equation (D2) result in

$$\frac{q^{1/3}}{T_w - T_b} \frac{1}{k^{1/3}} \left(\frac{\mu_l \lambda}{k_l} \right)^{2/3} Pr_l^{0.7} \left(\frac{\sigma}{\rho_l - \rho_v} \right)^{1/6} \frac{1}{g^{1/6}} = C_1 \tag{D2}$$

The fluid properties in equation (D2) are grouped so that the sensitivity of the equation to variation in fluid properties can be examined. Suppose this is done over a range of pressures from 40 to 140 pounds per square inch absolute, $0.2 < p/p_c < 0.8$, for saturation conditions. The significant properties for this pressure range are tabulated in the following table:

Property	Pressure, p, lb/sq in. abs		
	40	140	95
	Ratio of pressure to critical pressure, p/p_c		
	0.21	0.95	0.5
Heat capacity of liquid, c_l, Btu/(lb_m)(^oF)	2.9	5.8	4.0
Heat of vaporization, λ, Btu/lb	180	118	141
Dynamic viscosity, μ, lb_m/hr	6.7×10^{-6}	4.3×10^{-6}	5.0
Thermal conductivity, k, Btu/(ft)(hr)(^oF)	2.04×10^{-5}	2.3×10^{-5}	2.2×10^{-5}
Surface tension, σ, lb_f/ft	10.3×10^{-5}	6.4×10^{-5}	7.5
Density of liquid, ρ_l, lb_m/cu ft	4.10	3.15	3.56
Density of vapor, ρ_v, lb_m/cu ft	.21	.82	.52
Difference between liquid density and vapor density, $\rho_l - \rho_v$, lb_m/cu ft	3.89	2.33	3.04
Temperature, T, ^oR	43.5	55.8	57.5

By using the values in the preceding table, the ratio of equation (D2) at 40 pounds per square inch absolute to equation (D2) at 140 pounds per square inch absolute becomes

$$\left[\frac{\left(\frac{q^{1/3}}{\Delta T}\right)_{40 \text{ lb/sq in. abs}}}{\left(\frac{q^{1/3}}{\Delta T}\right)_{140 \text{ lb/sq in. abs}}}\right](1.8) = 1 \tag{D3}$$

where ΔT is $(T_w - T_b)$. If q is a constant, equation (D1) would predict:

$$\Delta T_{140 \text{ lb/sq in. abs}}(1.8) = \Delta T_{40 \text{ lb sq in. abs}} \tag{D4}$$

A similar exercise can be performed with the correlation of reference 20. The correlating equation is

$$\frac{hL}{k_l} = C_3\left[\left(\frac{p}{p_0}\right)\sqrt{\frac{c_l^2\rho_l^2}{M^2 P k_l \sigma \rho_v \lambda}}\, L^{3/2} q\right]^{2/3} \tag{D5}$$

Segregating the property terms and expressing h in terms of heat flux and driving temperature results in

$$\left(\frac{q^{1/3}}{\Delta T}\right)\left(\frac{1}{\rho_l k_l}\right)^{2/3}\left(\frac{\sigma \rho_v \lambda}{c_l}\right)^{1/3}\frac{1}{p^{2/3}} = \frac{C_3}{P^{1/3} M^{2/3} p_0^{2/3}} = C_4 \tag{D6}$$

If the properties listed in the previous table are used, the ratio of equation (D6) at 40 pounds per square inch absolute to equation (D6) at 140 pounds per square inch absolute becomes

$$\frac{\left(\frac{q^{1/3}}{\Delta T}\right)_{40 \text{ lb/sq in. abs}}}{\left(\frac{q^{1/3}}{\Delta T}\right)_{140 \text{ lb/sq in. abs}}}(2.25) = 1 \tag{D7}$$

If q is a constant, equation (D5) would be

$$\Delta T_{140 \text{ lb/sq in. abs}}(2.25) = \Delta T_{40 \text{ lb/sq in. abs}} \tag{D8}$$

It becomes rather obvious that both equations (D1) and (D5) are pressure sensitive and perhaps could predict the approximate values of ΔT once the level of heat transfer has been established. To compare the two equations, consider the data of figure 2 for q = constant = 0.0031 Btu per square inch per second listed in the following table:

Pressure, p, lb/sq in. abs	Temperature difference, ΔT	Equation	
		(D1)	(D5)
40	2.1	----	----
95	1.35	1.3	1.23
140	1.15	1.15	.9

It can be concluded from either of these equations that

$$q = K \cdot c(p)\Delta T^3$$

where $c(p)$ adjusts for saturation pressure variations and K adjusts the heat-transfer level. The latter, for the comparison, is a posteriori, and no apparent method becomes evident by the aforementioned exercise for predicting K a priori. Also, the experimental data indicate that the exponent on ΔT should be greater than three.

REFERENCES

1. Sherley, Joan E.: Nucleate Boiling Heat Transfer Data for Liquid Hydrogen at Standard and Zero Gravity. Advances in Cryogenic Eng., Vol. 8, Plenum Press, 1963, pp. 495-500.

2. Roubeau, P.: Exchanges Thermiques dans l'axote et l'hydrogene bouillant sous pression (Heat Transfer of Boiling Nitrogen and Hydrogen Under Pressure). Rep. 1877, Centre d'Etudes Nucleaires De Saclay (France), 1961, pp. 49-53.

3. Drayer, D. E., and Timmerhaus, K. D.: An Experimental Investigation of the Individual Boiling and Condensing Heat Transfer Coefficients for Hydrogen. Advances in Cryogenic Eng., Vol. 7, Plenum Press, 1961, pp. 401-412.

4. Richards, R. J., Steward, W. G., and Jacobs, R. B.: A Survey of the Literature on Heat Transfer from Solid Surfaces to Cryogenic Fluids. Tech. Note 122, NBS, Oct. 1961.

5. Westwater, J. W.: Nucleate Pool Boiling. Petroleum Management, vol. 33, no. 9, Aug. 1961, pp. 186-188.

6. Usiskin, C. M., and Siegel, R.: An Experimental Study of Boiling in Reduced and Zero Gravity Fields. Jour. Heat Transfer (Trans. ASME), ser. C, vol. 83, no. 3, Aug. 1961, pp. 243-253.

7. Merte, H., and Clark, J. A.: Boiling Heat Transfer Data for Liquid Nitrogen at Standard and Near-Zero Gravity. Advances in Cryogenic Eng., Vol. 7, Plenum Press, 1962, pp. 546-550.

8. Brazinsky, Irving, and Weiss, Solomon: A Photographic Study of Liquid Hydrogen Under Simulated Zero Gravity Conditions. NASA TM X-479, 1962.

9. Costello, C. P., and Adams, J. M.: Burnout Heat Fluxes in Pool Boiling at High Accelerations. Mech. Eng. Dept., Univ. Wash., 1960.

10. Merte, H., Jr., and Clark, J. A.: A Study of Pool Boiling in an Accelerating System. Tech. Rep. 3, College of Eng., Univ. Mich., Nov. 1959.

11. Ivey, H. J.: Acceleration and the Critical Heat Flux in Pool Boiling Heat Transfer. Proc. Instit. Mech. Eng., vol. 177, no. 1, 1963, pp. 15-42.

12. Adams, J. M.: A Study of the Critical Heat Flux in an Accelerating Pool Boiling System. Heat Transfer Lab., Univ. Wash., Sept. 1, 1962.

13. Graham, Robert W., and Hendricks, Robert C.: A Study of the Effect of Multi-G Accelerations on Nucleate-Boiling Ebullition. NASA TN D-1196, 1963.

14. Roder, Hans M., and Goodwin, Robert D.: Provisional Thermodynamic Functions for Para-Hydrogen. TN 130, NBS, Dec. 1961.

15. Griffith, J. D., and Sabersky, R. H.: Convection in a Fluid at Supercritical Pressures. ARS Jour., vol. 30, no. 3, Mar. 1960, pp. 289-291.

16. Holt, V. E., and Grosh, R. J.: Free Convection Heat Transfer up to Near-Critical Conditions. Nucleonics, vol. 21, no. 8, Aug. 1963, pp. 122-125.

17. Moore, Franklin D., and Mesler, Russell B.: The Measurement of Rapid Surface Temperature Flucuations During Nucleate Boiling of Water. A.I.Ch.E. Jour., vol. 7, no. 4, Dec. 1961, pp. 620-624.

18. Hendricks, R. C., and Sharp, R. R.: The Initiation of Cooling Due to Bubble Growth on a Heating Surface. NASA TN D-2290, 1964.

19. Hsu, Y. Y.: On the Size Range of Active Nucleation Cavities on a Heating Surface. Jour. Heat Transfer (Trans. ASME), ser. C, vol. 84, no. 3, Aug. 1962, pp. 207-216.

20. Yamagata, Kiyoshi, Hirano, Fujio, Nishikawa, Kanajasw, and Matsuoka, Hisamitsu: Nucleate Boiling of Water on the Horizontal Heating Surface. Faculty of Eng., Memoirs, Kyushu Univ., vol. 15, no. 1, 1955, pp. 97-163.

21. Rohsenow, W. M.: A Method of Correlating Heat-Transfer Data for Surface Boiling of Liquids. Trans. ASME, vol. 74, no. 6, Aug. 1952, pp. 969-976.

22. Zuber, N.: Nucleate Boiling. The Region of Isolated Bubbles and the Similarity with Natural Convection. Int. Jour. Heat and Mass Trans., vol. 6, no. 1, Jan. 1963, pp. 53-78.

23. Sharp, Robert R.: The Nature of Liquid Film Evaporation During Nucleate Boiling. NASA TN D-1997, 1964.

24. Deissler, R. G.: Heat Transfer and Fluid Friction for Fully Developed Turbulent Flow of Air and Supercritical Water with Variable Fluid Properties. Trans. ASME, vol. 76, no. 1, Jan. 1954, pp. 73-85. (See Discussion by Kurt Goldmann, p. 84.)

25. Johnson, Victor J.: A Compendum of the Properties of Materials at Low Temperature, Phase I. Final Rep., NBS, Dec. 1951, figure 3.281.

TABLE I. - DATA TABULATIONS FOR 0.006-INCH-THICK CHROMEL A HEATER

[When temperature difference across heater thickness is small compared to absolute temperature, value of column 4 is utilized.]

Run		Pressure, p, lb/sq in. abs	Temperature, T, ^{o}R	Difference between wall and bulk temperatures as read, $T_w - T_b$, ^{o}R	Heat flux, q, Btu/(sq in.)(sec)	Number of g's, n	Temperature difference, ΔT, ^{o}R
1	30	42.9	44.60	0.60	0.0010	1.00	0.56
2	31	43.2	44.60	3.70	0.0061	1.00	3.45
3	32	43.4	44.60	2.90	0.0138	1.00	2.32
4	33	43.3	44.90	3.60	0.0280	1.00	2.45
5	34	43.4	45.00	4.60	0.0330	1.00	3.26
6	35	43.9	45.10	5.00	0.0450	1.00	3.18
7	36	43.9	45.00	5.40	0.0600	1.00	2.98
8	37	44.0	45.10	5.80	0.0730	1.00	2.87
9	38	43.7	45.10	6.90	0.0980	1.00	3.02
10	39	43.9	45.10	8.80	0.1160	1.00	4.29
11	40	44.3	45.30	219.00	0.1300	1.00	219.00
12	41	43.6	45.90	10.00	0.0740	1.00	7.20
13	42	43.7	45.50	5.50	0.0470	1.00	3.63
14	43	43.5	45.40	4.20	0.0260	1.00	3.15
15	44	43.2	45.40	2.70	0.0120	1.00	2.21
16	45	43.3	45.50	1.20	0.0018	1.00	1.12
1	2847	47.8	44.80	1.46	0.0007	1.00	1.43
2	2848	47.8	44.90	2.47	0.0023	1.00	2.37
3	2849	48.1	44.90	2.87	0.0047	1.00	2.67
4	2850	47.8	44.90	3.15	0.0082	1.00	2.81
5	2851	47.9	44.90	4.03	0.0160	1.00	3.37
6	2852	48.0	44.90	4.86	0.0280	1.00	3.72
7	2853	48.3	45.00	5.43	0.0410	1.00	3.78
8	2854	48.6	45.00	5.96	0.0550	1.00	3.75
9	2855	48.6	45.00	6.41	0.0730	1.00	3.50
10	2856	48.6	45.10	6.75	0.0830	1.00	3.46
11	2857	48.6	45.00	4.55	0.0450	1.00	2.72
12	2858	48.1	45.00	1.66	0.0011	1.00	1.62

TABLE I. - Continued. DATA TABULATIONS FOR 0.006-INCH-THICK CHROMEL A HEATER

[When temperature difference across heater thickness is small compared to absolute temperature, value of column 4 is utilized.]

Run	Pressure, p, lb/sq in. abs	Temperature, T, °R	Difference between wall and bulk temperature as read, $T_w - T_b$, °R	Heat flux, q, Btu/(sq in.)(sec)	Number of g's, n	Temperature difference, ΔT, °R
1 2983	48.8	45.78	2.29	0.0056	1.00	2.06
2 2984	48.9	45.73	4.69	0.0312	1.00	3.45
3 2985	49.3	46.57	6.61	0.0718	1.00	3.84
4 2986	49.8	45.91	7.15	0.0859	1.00	3.81
5 2987	50.1	45.98	147.46	0.1010	1.00	147.46
6 2988	50.2	46.01	162.95	0.1112	1.00	162.95
7 2989	50.5	45.98	176.99	0.1208	1.00	176.99
8 2990	50.3	46.05	183.04	0.1261	1.00	183.04
9 2991	50.1	46.07	189.25	0.1297	1.00	189.25
10 2992	50.3	45.98	183.10	0.1233	1.00	183.10
11 2993	50.1	45.98	177.48	0.1206	1.00	177.48
12 2994	50.4	45.98	171.00	0.1161	1.00	171.00
13 2995	50.1	46.06	164.93	0.1119	1.00	164.93
14 2996	50.2	45.98	156.06	0.1057	1.00	156.06
15 2997	50.0	46.01	146.16	0.0982	1.00	146.16
16 2998	50.0	45.92	137.30	0.0927	1.00	137.30
17 2999	49.7	45.91	125.68	0.0839	1.00	125.68
18 3000	49.3	45.92	6.47	0.0731	1.00	3.61
19 3001	49.5	45.89	5.76	0.0605	1.00	3.38
20 3002	49.5	45.87	5.24	0.0507	1.00	3.23
21 3003	49.2	45.84	4.95	0.0445	1.00	3.18
1 2822	51.5	45.60	0.67	0.0006	7.30	0.65
2 2823	51.5	45.60	2.87	0.0023	7.30	2.78
3 2824	51.5	45.60	3.00	0.0050	7.30	2.80
4 2825	51.5	45.60	3.76	0.0091	7.30	3.39
5 2826	51.5	45.60	3.87	0.0160	7.30	3.22
6 2827	51.5	45.60	4.73	0.0270	7.50	3.65
7 2828	51.5	45.60	5.51	0.0390	7.50	3.96
8 2829	51.5	45.60	5.88	0.0540	7.70	3.74
9 2830	51.5	45.60	6.34	0.0650	7.70	3.78
10 2831	51.5	45.50	4.96	0.0410	7.70	3.32
11 2832	51.5	45.60	1.86	0.0110	7.70	1.40
12 2836	51.5	45.50	0.20	0.0006	7.00	0.18
13 2837	51.5	45.60	0.94	0.0022	7.00	0.85
14 2838	51.5	45.55	2.04	0.0076	7.00	1.73
15 2839	51.5	45.60	2.70	0.0140	7.00	2.13
16 2840	51.5	45.55	3.73	0.0260	7.00	2.67
17 2841	51.5	45.60	5.09	0.0420	7.00	3.41
18 2842	51.5	45.60	6.17	0.0560	7.00	3.96
19 2843	51.5	45.60	6.42	0.0700	7.20	3.66

TABLE I. - Continued. DATA TABULATIONS FOR 0.006-INCH-THICK CHROMEL A HEATER

[When temperature difference across heater thickness is small compared to absolute temperature, value of column 4 is utilized.]

Run	Pressure, p, lb/sq in. abs	Temperature, T, °R	Difference between wall and bulk temperatures as read, $T_w - T_b$, °R	Heat flux, q, Btu/(sq in.)(sec)	Number of g's, n	Temperature difference, ΔT, °R
1 2807	52.2	45.70	2.39	0.0014	1.00	2.34
2 2808	52.1	45.70	1.78	0.0036	1.00	1.63
3 2809	52.4	45.70	2.26	0.0075	1.00	1.95
4 2810	52.4	45.70	2.98	0.0130	1.00	2.45
5 2811	52.4	45.70	3.91	0.0220	1.00	3.02
6 2812	52.4	45.70	4.66	0.0360	1.00	3.22
7 2813	52.6	45.70	5.26	0.0500	1.00	3.27
8 2814	52.6	45.70	5.77	0.0670	1.00	3.12
9 2815	52.6	45.70	6.21	0.0810	1.00	3.02
10 2816	52.6	45.70	6.52	0.0930	1.00	2.87
11 2817	52.5	45.70	4.38	0.0500	1.00	2.37
12 2818	52.2	45.70	1.55	0.0130	1.00	1.01
1 3006	51.6	46.35	3.30	0.0080	7.10	2.98
2 3007	51.8	46.41	4.79	0.0337	7.10	3.47
3 3008	52.0	46.47	5.66	0.0530	7.10	3.59
4 3009	52.2	46.50	6.40	0.0678	7.10	3.77
5 3010	52.4	46.47	6.78	0.0802	7.10	3.68
6 3011	52.3	46.52	7.39	0.0908	7.10	3.91
7 3012	52.5	46.52	7.61	0.0952	7.10	3.97
8 3013	52.4	46.52	130.24	0.1047	7.10	130.24
9 3014	52.4	46.59	139.85	0.1071	7.10	139.85
10 3015	52.4	46.52	148.58	0.1144	7.10	148.58
11 3016	52.5	46.49	152.73	0.1180	7.10	152.73
12 3017	52.3	46.50	145.39	0.1126	7.10	145.39
13 3018	52.7	46.56	142.22	0.1091	7.10	142.22
14 3019	52.5	46.54	135.43	0.1043	7.10	135.43
15 3020	52.6	46.77	121.49	0.0934	7.10	121.49
16 3021	52.2	46.83	108.69	0.0826	7.10	108.69
17 3022	52.4	46.77	6.70	0.0735	7.10	3.88
18 3023	52.6	46.71	6.13	0.0624	7.10	3.72
19 3024	52.4	46.62	5.64	0.0522	7.78	3.61
1 2972	51.8	46.32	2.50	0.0026	1.00	2.39
2 2973	52.0	46.41	4.93	0.0330	1.00	3.63
3 2974	52.6	46.44	6.53	0.0778	1.00	3.53
4 2975	52.6	46.50	6.74	0.0866	1.00	3.41
5 2976	52.9	47.35	143.75	0.0993	1.00	143.75
6 2977	52.8	47.69	163.12	0.1125	1.00	163.12
7 2978	53.2	47.87	175.23	0.1201	1.00	175.23
8 2979	53.3	48.27	185.39	0.1269	1.00	185.39

TABLE I. - Continued. DATA TABULATIONS FOR 0.006-INCH-THICK CHROMEL A HEATER

[When temperature difference across heater thickness is small compared to absolute temperature, value of column 4 is utilized.]

Run		Pressure, p, lb/sq in. abs	Temperature, T, °R	Difference between wall and bulk temperatures as read, $T_w - T_b$, °R	Heat flux, q, Btu/(sq in.)(sec)	Number of g's, n	Temperature difference, ΔT, °R
1	48	66.5	48.80	2.10	0.0013	1.00	2.05
2	49	67.0	48.90	2.70	0.0087	1.00	2.37
3	50	67.5	48.90	2.80	0.0170	1.00	2.15
4	51	67.6	48.90	3.20	0.0320	1.00	1.98
5	52	68.1	49.10	3.70	0.0530	1.00	1.70
6	53	68.4	49.00	4.40	0.0680	1.00	1.84
7	54	68.4	49.10	11.90	0.0860	1.00	8.88
8	55	68.9	49.10	167.20	0.0960	1.00	167.20
9	56	68.7	49.10	133.10	0.0750	1.00	133.10
10	57	68.2	49.00	5.10	0.0610	1.00	2.82
11	58	68.1	49.00	3.10	0.0440	1.00	1.43
12	59	67.9	49.00	2.40	0.0260	1.00	1.40
13	60	67.8	49.00	1.70	0.0140	1.00	1.16
14	61	67.6	49.00	1.20	0.0072	1.00	0.92
15	62	67.6	48.90	0.50	0.0018	1.00	0.43
1	2683	74.6	49.13	1.16	0.0011	1.00	1.11
2	2684	74.8	49.13	1.42	0.0027	1.00	1.32
3	2685	74.1	49.26	1.92	0.0053	1.00	1.71
4	2686	74.7	49.18	2.61	0.0102	1.00	2.22
5	2687	74.3	49.33	2.94	0.0163	1.00	2.32
6	2689	74.5	49.34	3.84	0.0254	1.00	2.89
7	2690	74.8	49.40	4.25	0.0456	1.00	2.55
8	2691	74.5	49.45	4.72	0.0590	1.00	2.52
9	2692	74.5	49.59	4.73	0.0660	1.00	2.29
10	2693	74.6	49.59	4.96	0.0750	1.00	2.19
11	2694	74.7	49.63	5.52	0.0860	1.00	2.36
12	2695	74.3	49.67	6.26	0.0903	1.00	2.97
13	2696	74.0	49.60	3.35	0.0403	1.00	1.84
14	2697	73.6	49.56	1.74	0.0171	1.00	1.09
15	2698	73.9	49.46	0.72	0.0049	1.00	0.53

TABLE I. - Continued. DATA TABULATIONS FOR 0.006-INCH-THICK CHROMEL A HEATER

[When temperature difference across heater thickness is small compared to absolute temperature, value of column 4 is utilized.]

Run	Pressure, p, lb/sq in. abs	Temperature, T, °R	Difference between wall and bulk temperatures as read, $T_w - T_b$, °R	Heat flux, q, Btu/(sq in.)(sec)	Number of g's, n	Temperature difference, ΔT, °R
1 3120	77.1	50.78	2.85	0.0057	7.00	2.64
2 3121	76.8	50.72	2.71	0.0131	7.00	2.23
3 3122	76.7	50.75	2.97	0.0224	7.00	2.14
4 3123	76.3	50.75	3.67	0.0468	7.00	1.96
5 3124	76.2	50.81	4.92	0.0806	7.00	2.01
6 3125	76.0	50.84	5.61	0.0879	7.20	2.46
7 3126	76.1	50.81	120.83	0.0959	7.20	120.83
8 3127	76.0	50.78	133.24	0.1047	7.20	133.24
9 3128	76.1	50.84	149.29	0.1169	7.20	149.29
10 3129	76.0	50.81	164.94	0.1284	7.20	164.94
11 3130	75.8	50.75	180.90	0.1399	7.20	180.90
12 3131	75.7	50.81	159.12	0.1254	7.20	159.12
13 3132	75.7	50.78	149.88	0.1176	7.20	149.88
14 3133	75.7	50.75	131.94	0.1039	7.20	131.94
15 3134	75.5	50.77	110.38	0.0880	7.20	110.38
16 3135	75.6	50.81	98.77	0.0807	7.10	98.77
17 3137	75.5	50.78	3.10	0.0497	7.10	1.27
18 3138	75.4	50.72	2.14	0.0267	7.10	1.15
19 3139	75.3	50.68	1.34	0.0108	7.10	0.93
20 3140	75.2	50.66	0.56	0.0048	7.10	0.38
1 3100	89.7	51.66	2.32	0.0053	1.00	2.13
2 3101	89.4	51.60	2.48	0.0141	1.00	1.97
3 3102	89.3	51.59	3.27	0.0314	1.00	2.14
4 3103	89.5	51.64	4.00	0.0461	1.00	2.35
5 3104	89.3	51.57	4.57	0.0640	1.00	2.28
6 3105	89.4	51.59	5.64	0.0774	1.00	2.89
7 3106	89.2	51.57	126.62	0.0866	1.00	126.62
8 3107	89.2	51.62	142.23	0.0968	1.00	142.23
9 3108	88.9	51.59	154.87	0.1054	1.00	154.87
10 3109	88.8	51.62	169.75	0.1153	1.00	169.75
11 3110	88.6	51.58	154.41	0.1049	1.00	154.41
12 3111	88.4	51.51	139.35	0.0950	1.00	139.35
13 3112	88.2	51.45	117.37	0.0805	1.00	117.37
14 3113	87.9	51.48	72.42	0.0640	1.00	72.42
15 3114	87.5	51.44	4.30	0.0572	1.00	2.25
16 3115	87.3	51.37	3.85	0.0435	1.00	2.28
17 3116	87.1	51.39	2.80	0.0216	1.00	2.01
18 3117	86.6	51.30	1.56	0.0069	1.00	1.30

TABLE I. - Continued. DATA TABULATIONS FOR 0.006-INCH-THICK CHROMEL A HEATER

[When temperature difference across heater thickness is small compared to absolute temperature, value of column 4 is utilized.]

Run	Pressure, p, lb/sq in. abs	Temperature, T, °R	Difference between wall and bulk temperatures as read, $T_w - T_b$, °R	Heat flux, q, Btu/(sq in.)(sec)	Number of g's, n	Temperature difference, ΔT, °R
1 2525	89.7	52.50	1.40	0.0035	3.40	1.27
2 2526	89.8	52.50	1.96	0.0060	3.40	1.75
3 2528	89.6	52.50	2.47	0.0124	3.40	2.02
4 2529	89.7	52.50	2.98	0.0213	3.40	2.22
5 2530	89.6	52.50	3.50	0.0292	3.40	2.46
6 2531	89.6	52.50	4.02	0.0404	3.40	2.59
7 2532	89.6	52.40	4.53	0.0517	3.40	2.71
8 2533	89.7	52.50	5.56	0.0640	3.40	3.32
9 2534	89.6	52.50	7.11	0.0708	3.40	4.67
10 2535	89.3	52.50	4.03	0.0438	3.40	2.48
11 2536	89.4	52.40	2.95	0.0236	3.40	2.11
1 3046	90.2	52.08	2.03	0.0113	7.00	1.62
2 3047	90.4	52.14	3.10	0.0352	7.00	1.84
3 3048	90.3	52.21	4.06	0.0599	7.00	1.93
4 3049	90.4	52.14	4.39	0.0685	7.00	1.96
5 3050	90.1	52.11	5.34	0.0796	7.00	2.54
6 3051	90.2	52.07	116.11	0.0848	7.00	116.11
7 3052	90.6	52.08	125.35	0.0951	7.00	125.35
8 3053	90.7	52.08	122.72	0.0975	7.20	122.72
9 3054	90.5	52.14	137.89	0.1052	7.20	137.89
10 3055	90.6	52.07	132.14	0.0998	7.20	132.14
11 3056	90.8	51.95	126.05	0.0954	7.20	126.05
12 3057	90.5	51.96	112.68	0.0882	7.20	112.68
13 3058	90.5	52.03	100.83	0.0805	7.20	100.83
14 3059	90.9	52.05	92.71	0.0740	7.20	92.71
15 3060	90.8	52.14	23.43	0.0639	7.20	21.47
16 3061	90.7	52.02	4.65	0.0569	7.50	2.63
17 3062	90.9	52.08	4.50	0.0507	7.50	2.70
1 2863	90.9	51.30	0.31	0.0008	1.00	0.28
2 2864	91.0	51.30	0.77	0.0026	1.00	0.67
3 2865	90.9	51.30	1.59	0.0064	1.00	1.35
4 2366	91.1	51.40	1.87	0.0100	1.00	1.50
5 2867	91.1	51.40	2.44	0.0170	1.00	1.82
6 2868	91.2	51.40	3.00	0.0280	1.00	1.98
7 2869	91.2	51.40	3.61	0.0400	1.00	2.16
8 2870	91.4	51.40	3.94	0.0530	1.00	2.03
9 2871	91.5	51.50	4.33	0.0640	1.00	2.03
10 2872	91.5	51.50	5.22	0.0740	1.00	2.58

TABLE I. - Continued. DATA TABULATIONS FOR 0.006-INCH-THICK CHROMEL A HEATER

[When temperature difference across heater thickness is small compared to absolute temperature, value of column 4 is utilized.]

Run	Pressure, p, lb/sq in. abs	Temperature, T, °R	Difference between wall and bulk temperatures as read, $T_w - T_b$, °R	Heat flux, q, Btu/(sq in.)(sec)	Number of g's, n	Temperature difference, ΔT, °R
1 2876	91.5	51.70	0.22	0.0006	7.00	0.20
2 2877	91.5	51.70	1.82	0.0022	7.00	1.74
3 2878	91.5	51.70	2.08	0.0048	7.50	1.90
4 2879	91.5	51.80	1.95	0.0093	7.70	1.61
5 2880	91.5	51.70	2.28	0.0160	8.00	1.70
6 2881	91.5	51.70	2.69	0.0340	8.00	1.45
7 2882	91.5	51.70	2.94	0.0360	8.00	1.64
8 2883	91.5	51.70	3.33	0.0440	8.00	1.74
9 2884	91.5	51.80	3.56	0.0550	8.00	1.58
10 2885	91.5	51.90	4.16	0.0680	8.00	1.73
11 2889	91.5	51.70	0.20	0.0022	7.70	0.12
12 2890	91.5	51.80	0.62	0.0054	7.70	0.42
13 2891	91.5	51.70	1.19	0.0089	7.70	0.86
14 2892	91.5	51.70	1.97	0.0160	7.80	1.38
15 2893	91.5	51.80	2.60	0.0260	7.80	1.66
16 2894	91.5	51.80	3.06	0.0360	7.80	1.76
17 2895	91.5	51.80	3.64	0.0530	7.80	1.73
18 2896	91.5	51.90	3.99	0.0630	7.70	1.74
1 3027	92.1	52.07	2.09	0.0120	1.00	1.66
2 3028	92.1	52.02	3.08	0.0312	1.00	1.96
3 3029	92.4	52.05	3.42	0.0414	1.00	1.93
4 3030	92.3	52.05	4.20	0.0623	1.00	1.98
5 3031	92.2	52.14	5.28	0.0760	1.00	2.60
6 3032	92.2	52.02	123.04	0.0845	1.00	123.04
7 3033	92.4	52.05	130.07	0.0894	1.00	130.07
8 3034	92.2	51.99	139.00	0.0947	1.00	139.00
9 3035	92.3	52.02	148.13	0.1002	1.00	148.13
10 3036	92.2	52.04	160.88	0.1093	1.00	160.88
11 3037	92.0	51.93	152.92	0.1039	1.00	152.92
12 3038	92.3	52.11	145.24	0.0983	1.00	145.24
13 3039	92.0	52.10	135.38	0.0927	1.00	135.38
14 3040	92.1	52.02	121.62	0.0835	1.00	121.62
15 3041	91.8	52.05	112.36	0.0767	1.00	112.36
16 3042	91.6	51.97	96.80	0.0662	1.00	96.80
17 3043	91.6	52.07	4.12	0.0602	1.00	1.98

TABLE I. - Continued. DATA TABULATIONS FOR 0.006-INCH-THICK CHROMEL A HEATER

[When temperature difference across heater thickness is small compared to absolute temperature, value of column 4 is utilized.]

Run	Pressure, p, lb/sq in. abs	Temperature, T, °R	Difference between wall and bulk temperatures as read, $T_w - T_b$, °R	Heat flux, q, Btu/(sq in.)(sec)	Number of g's, n	Temperature difference, ΔT, °R
1 2500	93.8	52.80	0.98	0.0013	1.00	0.93
2 2501	93.6	52.80	1.07	0.0019	1.00	1.01
3 2502	93.5	52.80	1.34	0.0035	1.00	1.22
4 2503	93.6	52.80	1.51	0.0049	1.00	1.33
5 2504	93.5	52.70	1.93	0.0072	1.00	1.67
6 2505	93.6	52.70	1.91	0.0103	1.00	1.54
7 2506	93.5	52.70	2.42	0.0140	1.00	1.92
8 2507	93.2	52.70	2.56	0.0180	1.00	1.92
9 2509	93.3	52.70	3.17	0.0260	1.00	2.25
10 2512	93.3	52.60	3.74	0.0390	1.00	2.36
11 2513	93.0	52.70	3.82	0.0450	1.00	2.23
12 2515	92.9	52.60	4.69	0.0570	1.00	2.69
13 2517	92.9	52.70	7.22	0.0730	1.00	4.71
14 2518	93.1	52.70	4.00	0.0510	1.00	2.20
15 2519	92.8	52.70	2.87	0.0280	1.00	1.87
1 2549	94.2	53.40	0.87	0.0007	10.40	0.84
2 2550	94.0	53.40	1.65	0.0014	10.40	1.60
3 2551	94.2	53.40	2.04	0.0027	10.40	1.94
4 2552	94.3	53.40	1.87	0.0043	10.40	1.72
5 2553	94.3	53.40	1.83	0.0067	10.40	1.59
6 2554	94.4	53.40	1.84	0.0090	10.40	1.52
7 2555	94.2	53.40	2.13	0.0129	10.40	1.67
8 2556	94.5	53.40	2.28	0.0188	10.40	1.61
9 2557	94.5	53.40	2.63	0.0258	10.40	1.72
10 2558	94.6	53.50	2.93	0.0317	10.40	1.82
11 2559	95.0	53.50	3.50	0.0434	10.40	1.98
12 2560	95.0	53.50	3.88	0.0552	10.40	1.96
13 2561	95.0	53.50	4.78	0.0704	10.40	2.35
14 2562	95.0	53.50	7.82	0.0798	10.40	5.13
15 2563	95.1	53.50	3.59	0.0446	10.40	2.03
16 2564	95.0	53.40	2.37	0.0186	10.40	1.71
17 2565	95.0	53.40	1.48	0.0065	10.40	1.25

TABLE I. - Continued. DATA TABULATIONS FOR 0.006-INCH-THICK CHROMEL A HEATER

[When temperature difference across heater thickness is small compared to absolute temperature, value of column 4 is utilized.]

Run		Pressure, p, lb/sq in. abs	Temperature, T, ^{o}R	Difference between wall and bulk temperatures as read, $T_w - T_b$, ^{o}R	Heat flux, q, Btu/(sq in.)(sec)	Number of g's, n	Temperature difference, ΔT, ^{o}R
1	12	96.4	51.60	1.00	0.0023	10.00	0.91
2	13	96.3	51.70	1.70	0.0071	10.00	1.44
3	14	96.4	52.00	2.00	0.0127	10.00	1.54
4	15	96.7	52.10	2.40	0.0226	10.00	1.58
5	16	96.8	52.20	3.00	0.0350	10.00	1.74
6	17	96.9	52.10	3.20	0.0460	10.00	1.55
7	18	97.2	52.30	4.90	0.0600	10.00	2.78
8	20	98.2	52.00	176.70	0.1000	10.00	176.70
9	21	98.4	52.70	223.40	0.1220	10.00	223.40
10	22	98.2	52.70	163.30	0.0940	10.00	163.30
11	23	98.0	52.70	127.10	0.0670	10.00	127.10
12	24	97.7	52.80	3.30	0.0390	10.00	1.92
13	25	97.4	52.90	1.90	0.0230	10.00	1.08
14	26	97.2	52.70	0.80	0.0084	10.00	0.50
1	150	96.5	48.70	1.70	0.0005	1.00	1.68
2	151	96.5	48.80	2.90	0.0033	1.00	2.77
3	152	96.5	48.90	3.00	0.0123	1.00	2.53
4	153	96.5	49.20	4.80	0.0191	1.00	4.09
5	154	96.5	49.40	5.10	0.0330	1.00	3.88
6	155	96.5	49.60	6.10	0.0510	1.00	4.23
7	156	96.5	49.70	6.60	0.0590	1.00	4.45
8	157	96.5	49.90	8.70	0.0710	1.00	6.17
9	158	96.5	50.10	161.30	0.0960	1.00	161.30
10	159	96.5	50.20	127.90	0.0740	1.00	127.90
11	160	96.5	50.30	6.10	0.0540	1.00	4.15
12	161	96.5	50.40	4.40	0.0390	1.00	2.97
13	162	96.5	50.50	3.70	0.0240	1.00	2.82
14	163	96.5	50.50	3.60	0.0170	1.00	2.97
15	164	96.5	50.60	2.80	0.0098	1.00	2.44
16	165	96.5	50.60	1.30	0.0027	1.00	1.20
1	2715	96.9	52.92	1.34	0.0012	1.00	1.30
2	2717	96.8	52.82	1.89	0.0049	1.00	1.71
3	2718	97.3	52.80	1.99	0.0094	1.00	1.65
4	2719	97.2	52.92	2.33	0.0175	1.00	1.70
5	2720	97.5	52.89	2.68	0.0278	1.00	1.70
6	2721	97.9	52.89	3.10	0.0366	1.00	1.80
7	2722	97.7	52.94	3.55	0.0491	1.00	1.81
8	2723	97.6	52.94	3.90	0.0588	1.00	1.83
9	2724	98.1	52.92	4.19	0.0633	1.00	1.97

TABLE I. - Continued. DATA TABULATIONS FOR 0.006-INCH-THICK CHROMEL A HEATER

[When temperature difference across heater thickness is small compared to absolute temperature, value of column 4 is utilized.]

Run	Pressure, p, lb/sq in. abs	Temperature, T, °R	Difference between wall and bulk temperatures as read, $T_w - T_b$, °R	Heat flux, q, Btu/(sq in.)(sec)	Number of g's, n	Temperature difference, ΔT, °R
1 2730	122.0	55.41	0.84	0.0013	7.60	0.80
2 2731	121.4	55.49	0.90	0.0040	7.70	0.76
3 2732	121.7	55.52	0.92	0.0070	7.70	0.68
4 2733	121.5	55.55	0.88	0.0097	7.70	0.54
5 2734	121.7	55.69	1.23	0.0141	7.70	0.75
6 2735	121.4	55.66	1.55	0.0222	7.70	0.79
7 2736	122.0	55.66	2.02	0.0328	8.00	0.90
8 2737	122.0	55.76	2.24	0.0433	8.00	0.77
9 2738	121.4	55.86	3.00	0.0521	8.00	1.24
10 2739	121.9	55.83	3.73	0.0568	8.00	1.82
11 2740	121.7	55.72	2.94	0.0417	8.00	1.53
12 2741	121.7	55.76	1.87	0.0236	8.00	1.07
13 2742	121.2	55.83	1.31	0.0056	8.00	1.12
1 2745	123.6	52.01	1.39	0.0015	1.00	1.33
2 2746	123.6	52.12	2.41	0.0036	1.00	2.28
3 2747	123.5	52.27	2.92	0.0065	1.00	2.68
4 2748	123.6	52.50	3.52	0.0013	1.00	3.47
5 2749	124.0	52.60	3.83	0.0022	1.00	3.76
6 2750	124.0	52.73	3.91	0.0337	1.00	2.72
7 2751	124.0	52.94	4.32	0.0430	1.00	2.82
8 2752	123.8	53.10	5.51	0.0530	1.00	3.68
9 2753	124.2	53.23	10.39	0.0650	1.00	8.23
10 2758	122.3	54.49	0.71	0.0016	1.00	0.65
11 2759	122.7	54.55	1.10	0.0044	1.00	0.94
12 2760	122.7	54.52	1.30	0.0079	1.00	1.02
13 2761	122.7	54.58	1.66	0.0112	1.00	1.27
14 2762	122.9	54.66	2.10	0.0173	1.00	1.50
15 2763	122.7	54.74	2.90	0.0275	1.00	1.96
16 2764	122.9	54.76	4.03	0.0370	1.00	2.77
17 2765	122.4	54.91	5.67	0.0470	1.00	4.09
18 2766	122.7	54.85	7.33	0.0550	1.00	5.51
19 2767	122.6	54.95	11.62	0.0630	1.00	9.60

TABLE I. - Continued. DATA TABULATIONS FOR 0.006-INCH-

THICK CHROMEL A HEATER

[When temperature difference across heater thickness is small compared to absolute temperature, value of column 4 is utilized.]

Run		Pressure, p, lb/sq in. abs	Temperature, T, °R	Difference between wall and bulk temperatures as read, $T_w - T_b$, °R	Heat flux, q, Btu/(sq in.)(sec)	Number of g's, n	Temperature difference, ΔT, °R
1	65	131.6	55.40	0.60	0.0009	1.00	0.57
2	66	131.7	55.50	1.70	0.0074	1.00	1.45
3	67	131.9	55.60	2.00	0.0180	1.00	1.33
4	68	131.9	55.70	2.20	0.0230	1.00	1.42
5	69	132.2	55.70	3.30	0.0330	1.00	2.19
6	70	132.6	55.50	9.00	0.0560	1.00	7.19
7	71	132.7	55.90	10.80	0.0650	1.00	8.73
8	72	132.6	55.90	9.50	0.0530	1.00	7.80
9	75	132.1	56.00	2.20	0.0220	1.00	1.45
10	76	132.2	56.10	1.50	0.0110	1.00	1.13
11	77	132.0	56.00	1.20	0.0045	1.00	1.05
12	78	131.9	56.10	0.50	0.0017	1.00	0.44
1	3081	168.6	59.19	17.89	0.0120	1.00	17.55
2	3082	169.3	59.16	89.05	0.0398	1.00	89.05
3	3083	169.4	59.14	114.49	0.0474	1.00	114.49
4	3084	169.8	59.27	137.72	0.0514	1.00	137.72
5	3085	169.8	59.24	167.13	0.0618	1.00	167.13
6	3086	169.7	59.30	184.67	0.0685	1.00	184.67
7	3090	170.0	59.24	179.61	0.0689	1.00	179.61
8	3091	169.7	59.27	152.47	0.0599	1.00	152.47
9	3092	169.7	59.29	132.47	0.0521	1.00	132.47
10	3093	169.5	59.30	113.22	0.0453	1.00	113.22
11	3094	169.5	59.29	97.07	0.0401	1.00	97.07
12	3095	169.6	59.27	82.16	0.0360	1.00	82.16
13	3096	169.4	59.33	63.20	0.0291	1.00	63.20
14	3097	169.3	59.25	43.78	0.0229	1.00	43.78
1	3171	167.8	57.98	24.47	0.0151	1.00	24.04
2	3172	168.2	58.04	46.36	0.0259	1.00	46.36
3	3173	168.6	58.16	80.11	0.0400	1.00	80.11
4	3174	168.8	58.34	117.87	0.0517	1.00	117.87
5	3175	166.9	58.38	154.72	0.0622	1.00	154.72
6	3176	169.4	58.43	175.54	0.0721	1.00	175.54
7	3182	170.1	59.08	181.14	0.0728	1.00	181.14
8	3183	170.1	59.08	139.91	0.0550	1.00	139.91
9	3184	169.9	59.19	101.10	0.0442	1.00	101.10
10	3185	170.0	59.27	48.61	0.0256	1.00	48.61
11	3186	170.0	59.23	17.82	0.0116	1.00	17.48
12	3187	169.9	59.19	0.21	0.0057	1.00	0.02

TABLE I. - Continued. DATA TABULATIONS FOR 0.006-INCH-THICK CHROMEL A HEATER

[When temperature difference across heater thickness is small compared to absolute temperature, value of column 4 is utilized.]

Run		Pressure, p, lb/sq in. abs	Temperature, T, °R	Difference between wall and bulk temperatures as read, $T_w - T_b$, °R	Heat flux, q, Btu/(sq in.)(sec)	Number of g's, n	Temperature difference, ΔT, °R
1	3065	169.5	59.13	13.29	0.0106	7.80	12.98
2	3066	169.7	59.22	87.95	0.0381	7.80	87.95
3	3067	169.5	59.15	84.33	0.0450	7.80	84.33
4	3068	169.8	59.23	105.85	0.0548	7.80	105.85
5	3069	169.5	59.19	107.12	0.0619	7.80	107.12
6	3070	169.9	59.19	141.49	0.0703	7.80	141.49
7	3071	169.9	59.27	153.87	0.0788	7.80	153.87
8	3072	169.6	59.61	168.81	0.0856	7.80	168.81
9	3073	169.3	59.86	132.73	0.0633	7.80	132.73
10	3075	169.1	60.40	108.94	0.0496	7.80	108.94
11	3076	168.9	60.44	101.88	0.0454	7.80	101.88
12	3077	168.8	60.71	90.17	0.0394	7.80	90.17
13	3078	168.8	60.84	81.17	0.0350	7.80	81.17
1	81	174.0	58.70	0.60	0.0017	1.00	0.55
2	82	174.1	58.70	0.90	0.0040	1.00	0.77
3	83	174.1	58.70	1.40	0.0064	1.00	1.19
4	84	174.1	58.80	11.20	0.0121	1.00	10.83
5	96	174.6	58.90	18.70	0.0200	1.00	18.12
6	86	174.9	58.90	59.70	0.0260	1.00	59.70
7	87	174.8	59.00	96.60	0.0350	1.00	96.60
8	88	174.7	59.10	57.00	0.0230	1.00	57.00
9	89	174.6	59.00	36.40	0.0180	1.00	35.92
10	90	174.6	59.20	10.70	0.0120	1.00	10.33
11	91	174.5	59.20	3.20	0.0094	1.00	2.90
12	92	174.4	59.10	0.80	0.0067	1.00	0.58
13	93	174.5	59.20	0.40	0.0012	1.00	0.36

TABLE I. - Continued. DATA TABULATIONS FOR 0.006-INCH-THICK CHROMEL A HEATER

[When temperature difference across heater thickness is small compared to absolute temperature, value of column 4 is utilized.]

Run		Pressure, p, lb/sq in. abs	Temperature, T, °R	Difference between wall and bulk temperatures as read, $T_w - T_b$, °R	Heat flux, q, Btu/(sq in.)(sec)	Number of g's, n	Temperature difference, ΔT, °R
1	185	182.3	55.60	3.30	0.0015	1.00	3.25
2	186	182.3	55.60	4.80	0.0069	1.00	4.57
3	187	182.3	55.60	6.65	0.0100	1.00	6.32
4	188	182.3	55.80	39.60	0.0200	1.00	39.06
5	189	182.3	55.90	50.30	0.0230	1.00	50.30
6	190	182.3	56.00	71.20	0.0270	1.00	71.20
7	191	182.3	56.10	105.80	0.0370	1.00	105.80
8	192	182.3	56.20	154.70	0.0540	1.00	154.70
9	193	182.3	56.40	189.30	0.0650	1.00	189.30
10	194	182.3	56.80	150.80	0.0530	1.00	150.80
11	195	182.0	56.80	125.40	0.0430	1.00	125.40
12	196	182.0	56.80	87.50	0.0330	1.00	87.50
13	197	182.0	56.80	56.00	0.0220	1.00	56.00
14	198	181.7	56.80	10.45	0.0120	1.00	10.07
15	199	181.7	57.00	2.45	0.0064	1.00	2.24
16	200	181.4	57.00	1.70	0.0023	1.00	1.62
1	73	190.8	56.30	1.40	0.0017	1.00	1.34
2	74	190.8	56.40	23.60	0.0100	1.00	23.31
3	75	190.8	56.40	64.10	0.0240	1.00	64.10
4	76	190.8	56.50	134.50	0.0490	1.00	134.50
5	77	190.8	56.60	183.00	0.0660	1.00	183.00
6	80	190.8	57.20	234.60	0.0850	1.00	234.60
1	98	194.4	56.40	2.30	0.0016	1.00	2.25
2	99	194.4	56.50	3.20	0.0045	1.00	3.05
3	100	194.4	56.50	19.30	0.0099	1.00	19.00
4	101	194.4	56.60	41.50	0.0170	1.00	41.05
5	102	194.4	56.80	78.90	0.0300	1.00	78.90
6	103	194.4	56.90	115.50	0.0420	1.00	115.50
7	104	194.4	57.10	158.20	0.0550	1.00	158.20
8	105	194.4	57.20	110.40	0.0410	1.00	110.40
1	3200	211.8	55.46	3.95	0.0021	7.80	3.88
2	3201	212.3	55.65	7.51	0.0072	7.80	7.27
3	3202	212.2	55.86	22.02	0.0230	7.80	21.34
4	3203	212.5	56.29	44.53	0.0415	7.80	44.53
5	3204	212.6	56.65	78.08	0.0658	7.80	78.08
6	3205	212.8	56.98	110.33	0.0896	7.80	110.33

TABLE I. - Continued. DATA TABULATIONS FOR 0.006-INCH-THICK CHROMEL A HEATER

[When temperature difference across heater thickness is small compared to absolute temperature, value of column 4 is utilized.]

Run		Pressure, p, lb/sq in. abs	Temperature, T, °R	Difference between wall and bulk temperatures as read, $T_w - T_b$, °R	Heat flux, q, Btu/(sq in.)(sec)	Number of g's, n	Temperature difference, ΔT, °R
1	202	212.9	60.20	1.40	0.0013	1.00	1.36
2	203	212.9	60.30	5.20	0.0039	1.00	5.08
3	204	212.9	60.40	13.30	0.0079	1.00	13.07
4	205	212.9	60.40	30.90	0.0173	1.00	30.44
5	206	212.9	60.50	52.20	0.0259	1.00	52.20
6	207	212.9	60.50	90.20	0.0384	1.00	90.20
7	208	212.9	60.50	133.80	0.0518	1.00	133.80
8	209	212.9	60.60	153.40	0.0637	1.00	153.40
9	210	212.9	60.60	88.10	0.0354	1.00	88.10
10	211	212.9	60.60	38.00	0.0160	1.00	37.59
1	214	214.1	54.30	3.50	0.0018	6.60	3.44
2	215	214.1	54.30	4.90	0.0042	6.60	4.76
3	216	214.1	54.30	7.20	0.0071	6.60	6.96
4	217	214.1	54.30	9.90	0.0093	6.60	9.59
5	218	214.1	54.30	14.70	0.0142	6.60	14.25
6	219	214.1	54.30	26.90	0.0225	6.60	26.24
7	220	214.1	54.30	41.70	0.0315	6.60	40.85
8	221	214.1	54.30	54.50	0.0407	6.60	54.50
9	222	214.1	54.30	70.20	0.0503	6.60	70.20
10	223	214.1	54.30	84.20	0.0586	6.60	84.20
11	224	214.1	54.30	96.10	0.0675	6.60	96.10
12	225	214.1	54.30	115.50	0.0823	6.60	115.50
13	226	214.1	54.40	133.80	0.0944	6.60	133.80
14	227	214.1	54.40	70.50	0.0496	6.60	70.50
15	228	215.6	54.40	26.30	0.0223	7.00	25.65
1	3190	216.0	52.30	8.86	0.0067	1.00	8.64
2	3191	217.0	52.53	24.75	0.0138	1.00	24.33
3	3192	217.0	52.60	42.98	0.0231	1.00	42.35
4	3193	216.8	52.72	70.46	0.0358	1.00	70.46
5	3194	216.6	52.89	87.97	0.0439	1.00	87.97
6	3195	216.5	53.08	113.16	0.0551	1.00	113.16
7	3196	216.4	53.19	91.07	0.0450	1.00	91.07
8	3197	216.6	53.45	31.28	0.0171	1.00	30.78

TABLE I. - Concluded. DATA TABULATIONS FOR 0.006-INCH-THICK CHROMEL A HEATER

[When temperature difference across heater thickness is small compared to absolute temperature, value of column 4 is utilized.]

Run		Pressure, p, lb/sq in. abs	Temperature, T, °R	Difference between wall and bulk temperatures as read, $T_w - T_b$, °R	Heat flux, q, Btu/(sq in.)(sec)	Number of g's, n	Temperature difference, ΔT, °R
1	3208	216.3	55.78	11.35	0.0072	1.00	11.13
2	3209	217.0	55.92	43.71	0.0238	1.00	43.09
3	3210	217.7	55.92	82.72	0.0414	1.00	82.72
4	3211	217.8	55.98	108.54	0.0529	1.00	108.54
5	3212	217.7	56.15	124.96	0.0599	1.00	124.96
6	3213	217.3	56.21	46.06	0.0243	1.00	46.06
1	232	258.2	58.70	1.50	0.0016	7.00	1.45
2	233	258.2	58.70	3.50	0.0036	7.00	3.38
3	234	258.2	58.70	6.00	0.0064	7.00	5.80
4	235	258.2	58.70	10.00	0.0099	7.00	9.70
5	236	258.2	58.80	16.90	0.0156	7.00	16.44
6	237	258.2	58.80	26.90	0.0227	7.00	26.27
7	238	258.2	58.80	45.20	0.0357	7.00	45.20
8	239	258.2	58.80	63.20	0.0484	7.00	63.20
9	240	258.2	58.90	84.70	0.0628	7.00	84.70
10	241	258.2	58.90	114.80	0.0834	7.00	114.80
11	242	260.6	59.10	134.60	0.0969	7.30	134.60
1	245	266.0	60.40	3.60	0.0015	7.30	3.55
2	246	266.0	60.50	5.30	0.0028	7.30	5.21
3	247	266.0	60.50	9.70	0.0054	7.30	9.54
4	248	266.0	60.60	17.60	0.0090	7.30	17.34
5	249	266.0	60.70	28.30	0.0146	7.30	27.91
6	250	266.0	60.70	50.80	0.0240	7.30	50.80
7	251	266.0	60.80	73.70	0.0331	7.30	73.70
8	252	266.0	60.80	99.00	0.0435	7.30	99.00
9	253	266.0	60.80	126.00	0.0552	7.30	126.00
10	254	266.0	60.80	145.50	0.0690	7.30	145.50

VK
2/6/85

"The aeronautical and space activities of the United States shall be conducted so as to contribute . . . to the expansion of human knowledge of phenomena in the atmosphere and space. The Administration shall provide for the widest practicable and appropriate dissemination of information concerning its activities and the results thereof."

—NATIONAL AERONAUTICS AND SPACE ACT OF 1958

NASA SCIENTIFIC AND TECHNICAL PUBLICATIONS

TECHNICAL REPORTS: Scientific and technical information considered important, complete, and a lasting contribution to existing knowledge.

TECHNICAL NOTES: Information less broad in scope but nevertheless of importance as a contribution to existing knowledge.

TECHNICAL MEMORANDUMS: Information receiving limited distribution because of preliminary data, security classification, or other reasons.

CONTRACTOR REPORTS: Technical information generated in connection with a NASA contract or grant and released under NASA auspices.

TECHNICAL TRANSLATIONS: Information published in a foreign language considered to merit NASA distribution in English.

TECHNICAL REPRINTS: Information derived from NASA activities and initially published in the form of journal articles.

SPECIAL PUBLICATIONS: Information derived from or of value to NASA activities but not necessarily reporting the results of individual NASA-programmed scientific efforts. Publications include conference proceedings, monographs, data compilations, handbooks, sourcebooks, and special bibliographies.

Details on the availability of these publications may be obtained from:

SCIENTIFIC AND TECHNICAL INFORMATION DIVISION

NATIONAL AERONAUTICS AND SPACE ADMINISTRATION

Washington, D.C. 20546